

Yukawa Textures with Enhanced Symmetries in Heterotic Calabi-Yau Compactifications

Jun Dong¹, Tatsuo Kobayashi¹, Shuhei Miyamoto¹, and Hajime Otsuka^{2,3}

¹*Department of Physics, Hokkaido University, Sapporo 060-0810, Japan*

²*Department of Physics, Kyushu University, 744 Motooka, Nishi-ku, Fukuoka 819-0395, Japan*

³*Quantum and Spacetime Research Institute (QuaSR), Kyushu University, 744 Motooka, Nishi-ku, Fukuoka, 819-0395, Japan*

E-mail: j-dong@particle.sci.hokudai.ac.jp,
kobayashi@particle.sci.hokudai.ac.jp,
s-miyamoto@particle.sci.hokudai.ac.jp,
otsuka.hajime@phys.kyushu-u.ac.jp

ABSTRACT: We clarify the structure of Yukawa couplings and mass matrices for matter fields in heterotic string theory on smooth Calabi-Yau threefolds with standard embedding. The topological structure of Calabi-Yau threefolds leads to interesting Yukawa textures that cannot be derived from group-theoretical symmetries, e.g., the so-called Weinberg texture in the case of two generations of matter fields. Furthermore, we find that a $U(2)$ flavor symmetry, which plays an important role in controlling higher-dimensional operators in the Standard Model effective field theory, emerges at specific loci in the moduli space of multi-Higgs fields. Small perturbations around these loci generate semi-realistic patterns of quark masses and mixings.

Contents

1	Introduction	1
2	Calabi-Yau compactifications and low energy effective field theory	2
3	Yukawa textures and mass hierarchies	4
3.1	Coupling selection rules and Yukawa textures	4
3.2	CICYs with $h^{1,1} = 2$	7
3.3	CICYs with $h^{1,1} = 3$	12
3.4	Phenomenological implications	17
4	Conclusions	23
A	$h^{1,1} = 3$	24

1 Introduction

String theory is a promising candidate for a unified theory of all fundamental interactions including gravity and matter fields such as quarks, leptons, and the Higgs boson. It is expected that string theory can solve various mysteries in particle physics and cosmology. Superstring theory predicts the existence of a six-dimensional compact space in addition to our four-dimensional spacetime. All properties of particle physics and cosmology in four-dimensional low-energy effective field theory are determined by the details of string compactifications.

The presence or absence of specific particle modes is governed by the behavior of the corresponding string states in the compact space. In addition, their allowed couplings as well as forbidden ones are controlled by string compactifications. That is known as *stringy coupling selection rules*. Moreover, the magnitudes of the couplings depend on geometrical parameters of the compact space. Stringy coupling selection rules can often be understood in terms of group theory. For example, heterotic orbifold models and intersecting/magnetized D-brane models lead to discrete flavor symmetry groups [1–7]. These discrete flavor symmetries are useful to understand the origin of flavor structures such as mass hierarchies of quarks and leptons and their mixing angles. (See Refs. [8–14] for bottom-up approaches based on discrete flavor symmetries.)

Also, in certain classes of heterotic orbifold models and intersecting/magnetized D-brane models, modular symmetries behave as flavor symmetries [15–30]. In addition, the modular symmetries act as flavor symmetries in heterotic string theory on Calabi-Yau (CY) manifolds [31–34]. These modular flavor symmetries also provide a useful framework for

understanding the origin of flavor structure. (See Refs. [35–39] for bottom-up approaches based on modular flavor symmetries.¹)

On the other hand, some of the stringy selection rules cannot be understood in terms of group-theoretical symmetries. For example, such stringy selection rules in heterotic orbifold models were studied in Refs. [42–44]. In particular, conjugacy classes of space groups play an essential role in determining the selection rules in heterotic orbifold models [45–53]. Similar structures arise in magnetized D-brane models on toroidal orbifolds [54, 55]. These structures correspond to hypergroups mathematically, and their selection rules are non-invertible. Recently, these selection rules, e.g. \mathbf{Z}_2 gauging of \mathbf{Z}_N symmetries, have been applied to particle physics, leading to interesting results, e.g. novel Yukawa textures of quarks and leptons [56–59], axion-less solutions to the strong CP problem [60–62], radiative seesaw models [63–66], suppression of flavor changing neutral currents [67], and the stability of dark matter [68, 69], which cannot be derived from group-theoretical symmetries.

Furthermore, heterotic string theory on CY manifolds leads to non-trivial selection rules. These selection rules are not governed by group-theoretical considerations, but rather by topological properties of the CY threefolds. When we consider the so-called standard embedding [70], one can extract the effective action of matter fields from the corresponding moduli fields.² Then, the allowed couplings of matter fields are determined by intersection numbers of the corresponding cycles. Recently, such selection rules have been systematically classified for complete intersection Calabi-Yau (CICY) manifolds with five or fewer moduli [74]. The structure of Yukawa textures for matter fields was also studied. It is important to further investigate the phenomenological implications of these textures. That is our purpose. In this paper, we study fermion mass hierarchies arising from heterotic Calabi-Yau compactifications with standard embedding with particular emphasis on the structure of Yukawa textures.

This paper is organized as follows. In section 2, we review the low-energy effective action of matter fields, in particular, their Kähler potential and Yukawa couplings, in heterotic string theory on CY threefolds with standard embedding. After reviewing the coupling selection rules of matter fields in section 3.1, we explicitly analyze their Yukawa textures and mass hierarchies for CICYs with $h^{1,1} = 2$ in section 3.2 and $h^{1,1} = 3$ in section 3.3. Realistic patterns of quark masses and mixings are demonstrated in section 3.4. Section 4 is devoted to the conclusions. In Appendix A, we summarize the Yukawa textures of matter fields for CICYs with $h^{1,1} = 3$.

2 Calabi-Yau compactifications and low energy effective field theory

In this section, we briefly review the low-energy effective action of heterotic string theory on smooth CY threefolds. In particular, we focus on the standard embedding, in which the four-dimensional gauge theory is described by $E_6 \times E'_8$. Since the $SU(3) \subset E_8$ bundle is identified

¹See for reviews of the bottom-up approaches to modular flavor models [40, 41].

²For the scenario of non-standard embedding, the quark masses and mixings have been studied in e.g., Refs. [71, 72] using machine-learning techniques. The hierarchical structure of quark masses has been obtained by using Froggatt–Nielsen mechanism [73].

with the tangent bundle of CY threefolds, the **27** fundamental and $\overline{\mathbf{27}}$ anti-fundamental representations of E_6 are in one-to-one correspondence with Kähler and complex structure moduli of CY threefolds, respectively. Hence, the low-energy effective action of these matter fields can be derived directly from those of corresponding moduli fields.

Following Ref. [75], let us consider the effective action of the matter fields $\mathbf{27}^a$, i.e., fundamental representation of E_6 , represented by A^a . When their field values are small, i.e., $|A^a| \ll 1$, the matter Kähler metric is described by

$$K_{a\bar{b}}^{(\mathbf{27})} = e^{\frac{1}{3}(K_{\text{cs}} - K_{\text{ks}})} (K_{\text{ks}})_{a\bar{b}}, \quad (2.1)$$

where K_{ks} and K_{cs} respectively denote the Kähler potential of Kähler and complex structure moduli:

$$\begin{aligned} K_{\text{ks}} &= -\ln \left[\frac{1}{6} \sum_{a,b,c} \kappa_{abc} (T^a + \bar{T}^a)(T^b + \bar{T}^b)(T^c + \bar{T}^c) \right], \\ K_{\text{cs}} &= -\ln \left[\frac{i}{6} \sum_{i,j,k} \kappa_{ijk} (U^i - \bar{U}^i)(U^j - \bar{U}^j)(U^k - \bar{U}^k) \right], \end{aligned} \quad (2.2)$$

with κ_{abc} and κ_{ijk} corresponding to intersection numbers. Here, we assume the large Kähler structure and complex structure regime such that loop and quantum corrections are sufficiently suppressed compared to the classical terms considered here. However, taking the Kähler moduli to be arbitrarily large is not consistent with the observed value of four-dimensional gauge coupling. From the low-energy effective action of Yang-Mills fields:

$$S_{\text{bos}} \supset -\frac{1}{2g_{10}^2} \int_{M^{(10)}} e^{-2\phi_{10}} \text{tr}(F \wedge *F), \quad (2.3)$$

with $g_{10}^2 = 2(2\pi)^7(\alpha')^3$ being the ten-dimensional gauge coupling, the four-dimensional gauge coupling g_4 is written in terms of the string coupling $g_s = e^{\langle\phi_{10}\rangle}$ and the CY volume in units of string length $l_s = 2\pi\sqrt{\alpha'}$, i.e., $\text{Vol}(\mathcal{M}) = \mathcal{V} l_s^6$:

$$\alpha^{-1} = \frac{4\pi}{g_4^2} = e^{-2\langle\phi_{10}\rangle} \frac{4\pi \text{Vol}(\mathcal{M})}{g_{10}^2} = g_s^{-2} \mathcal{V}, \quad (2.4)$$

where

$$\mathcal{V} = \frac{1}{48} \sum_{a,b,c} \kappa_{abc} (T^a + \bar{T}^a)(T^b + \bar{T}^b)(T^c + \bar{T}^c). \quad (2.5)$$

Hence, the four-dimensional gauge coupling at the scale of grand unified theory (GUT), $\alpha^{-1}(M_{\text{GUT}}) \simeq 25$ with $M_{\text{GUT}} \simeq 2 \times 10^{16}$ GeV, puts an upper bound on the CY volume:

$$\mathcal{V} = g_s^2 \alpha^{-1} \lesssim 25, \quad (2.6)$$

assuming a perturbative string coupling $g_s \lesssim 1$.

Furthermore, the three-point couplings of $\mathbf{27}$, i.e., the Yukawa interactions, are described by the following superpotential in terms of the intersection numbers [76, 77]:

$$W = \frac{1}{6} \kappa_{abc} A^a A^b A^c. \quad (2.7)$$

Then, physical Yukawa couplings can be obtained after canonically normalizing the matter fields. Note that the fields A^a include quarks and leptons as well as Higgs fields. As discussed above, the existence of hierarchical Yukawa structures depends on the texture of the holomorphic Yukawa couplings. For concreteness, we restrict our analysis to CICY classified in Refs. [78–82]. This class of CY threefolds is embedded in an ambient space, i.e., a product of complex projective spaces $\mathbb{P}^{n_1} \times \dots \times \mathbb{P}^{n_m}$. The following configuration matrix characterizes the CICYs:

$$\begin{array}{c} \mathbb{P}^{n_1} \\ \mathbb{P}^{n_2} \\ \vdots \\ \mathbb{P}^{n_m} \end{array} \begin{bmatrix} q_1^1 & q_2^1 & \cdots & q_R^1 \\ q_1^2 & q_2^2 & \cdots & q_R^2 \\ \vdots & \vdots & \ddots & \vdots \\ q_1^m & q_2^m & \cdots & q_R^m \end{bmatrix}, \quad (2.8)$$

which means that n^l and the positive integers q_r^l ($r = 1, \dots, R$, $l = 1, \dots, m$), specifying R multi-degrees of homogeneous polynomials, are restricted to satisfy the so-called CY condition:

$$\sum_{r=1}^R q_r^l = n_l + 1 \quad (\forall l), \quad \sum_{l=1}^m n_l = R + 3. \quad (2.9)$$

Among the total of 7890 CICYs³, in this paper, we focus on the CICYs whose second cohomology descends from that of the ambient space, namely the so-called favorable CICYs.

3 Yukawa textures and mass hierarchies

Here, we study Yukawa textures and mass hierarchies arising from heterotic string theory on CICYs with $h^{1,1} = 2, 3, 4$.

3.1 Coupling selection rules and Yukawa textures

In this section, we review the results of Ref. [74] concerning coupling selection rules and Yukawa textures derived from heterotic string theory on CICYs with $h^{1,1} = 2, 3, 4$. In Ref. [74], CICYs were classified by their intersection numbers κ_{abc} . In particular, it was systematically classified which intersection numbers κ_{abc} vanish. Table 1 shows this classification for $h^{1,1} = 2$. Note that Type 4 was missed in Ref. [74]. Table 2 lists concrete examples of CICYs, identified by their numbering in Ref. [84]. In addition, Table 3 shows possible Yukawa textures for two generations $A^{1,2}$ under the assumption that one of A^1 and A^2 corresponds to the Higgs field. Note that the texture of Type 2 with the Higgs field A^1 and the texture for Type 3 with the Higgs field A^2 cannot be realized by group-theoretical symmetries. For example, it is impossible to assign consistent $U(1)$ charges to the two generations to reproduce this texture. It is known as the Weinberg texture in the down sector [85], which can explain the Cabibbo angle by the mass ratio between m_d and m_s as $\sqrt{m_d/m_s}$.

³Note that some CICYs share the same topological properties [83].

Table 1: Types of prepotential for CICYs with $h^{1,1} = 2$. Vanishing $\kappa_{abc} = 0$ are shown.

Type	$\kappa_{abc} = 0$
1	none
2	$\kappa_{111} = 0$
3	$\kappa_{111} = \kappa_{112} = 0$
4	$\kappa_{111} = \kappa_{222} = 0$

Table 2: Types of concrete CICYs with $h^{1,1} = 2$.

Type	Number of CICY
1	7644, 7726, 7759, 7761, 7799, 7809, 7863
2	7643, 7668, 7725, 7758, 7807, 7808, 7821, 7833, 7844, 7853, 7868, 7883
3	7806, 7816, 7817, 7819, 7822, 7823, 7840, 7858, 7867, 7869, 7873, 7882, 7885, 7886, 7887, 7888
4	7884

Table 3: Yukawa textures from CICYs with $h^{1,1} = 2$.

Type \ Higgs field	A^1	A^2
Type 1	$\begin{pmatrix} * & * \\ * & * \end{pmatrix}$	$\begin{pmatrix} * & * \\ * & * \end{pmatrix}$
Type 2	$\begin{pmatrix} 0 & * \\ * & * \end{pmatrix}$	$\begin{pmatrix} * & * \\ * & * \end{pmatrix}$
Type 3	$\begin{pmatrix} 0 & 0 \\ 0 & * \end{pmatrix}$	$\begin{pmatrix} 0 & * \\ * & * \end{pmatrix}$
Type 4	$\begin{pmatrix} 0 & * \\ * & * \end{pmatrix}$	$\begin{pmatrix} * & * \\ * & 0 \end{pmatrix}$

Similarly, we can classify CICYs with $h^{1,1} = 3$ according to their intersection numbers. The results are summarized in Tables 4, 5, and 6, which are organized in the same manner as the corresponding tables for $h^{1,1} = 2$. From this classification, we obtain non-trivial Yukawa textures. It is notable that some of these textures cannot be reproduced by conventional group-theoretical symmetries.

Table 4: Types of prepotential for CICYs with $h^{1,1} = 3$. Vanishing κ_{abc} are shown.

Type	$\kappa_{abc} = 0$
1	$\kappa_{111}, \kappa_{222}, \kappa_{333}$
2	$\kappa_{111}, \kappa_{222}$
3	$\kappa_{111}, \kappa_{112}, \kappa_{113}$
4	$\kappa_{111}, \kappa_{112}, \kappa_{113}, \kappa_{222}$
5	κ_{111}
6	none
7	$\kappa_{111}, \kappa_{112}, \kappa_{113}, \kappa_{122}, \kappa_{222}, \kappa_{223}$
8	$\kappa_{111}, \kappa_{112}, \kappa_{113}, \kappa_{122}, \kappa_{222}$
9	$\kappa_{111}, \kappa_{112}, \kappa_{113}, \kappa_{222}, \kappa_{333}$
10	$\kappa_{111}, \kappa_{112}, \kappa_{113}, \kappa_{122}, \kappa_{222}, \kappa_{333}$
11	$\kappa_{111}, \kappa_{112}, \kappa_{113}, \kappa_{122}, \kappa_{222}, \kappa_{223}, \kappa_{333}$

Table 5: Types of concrete CICYs with $h^{1,1} = 3$.

Type	Number of CICY
1	5299, 6971, 7580, 7581, 7669, 7729, 7846
2	6220, 6555, 6827, 6972, 7143, 7235, 7240, 7365, 7366, 7369, 7486, 7534, 7583, 7612, 7646, 7698, 7762, 7791
3	6771, 7036, 7208, 7530, 7563, 7566, 7571, 7578, 7588, 7626, 7631, 7635, 7636, 7638, 7647, 7648, 7679, 7717, 7721, 7734, 7747, 7781, 7842
4	7069, 7316, 7317, 7452, 7464, 7485, 7556, 7558, 7561, 7562, 7570, 7584, 7585, 7587, 7610, 7627, 7645, 7676, 7697, 7710, 7711, 7720, 7730, 7752, 7755, 7763, 7798, 7802, 7824, 7843, 7847, 7854
5	7071, 7144, 7237, 7370, 7488, 7586
6	7242
7	7450, 7481, 7484, 7555, 7560, 7579, 7661, 7662, 7677, 7694, 7707, 7714, 7735, 7745, 7746, 7753, 7760, 7769, 7776, 7779, 7780, 7788, 7789, 7792, 7795, 7797, 7812, 7834, 7836, 7841, 7845, 7848, 7851, 7865, 7871, 7872, 7874, 7877, 7881
8	7465, 7466, 7565, 7576, 7577, 7637, 7678, 7680, 7712, 7713, 7756, 7774, 7782, 7783, 7787, 7801, 7804, 7832, 7838, 7855, 7866, 7876
9	7708, 7727, 7728, 7831, 7870
10	7875
11	7880

Table 6: Yukawa textures from CICYs with $h^{1,1} = 3$.

Type \ Higgs field	A^1	A^2	A^3
Type 1	$\begin{pmatrix} 0 & * & * \\ * & * & * \\ * & * & * \end{pmatrix}$	$\begin{pmatrix} * & * & * \\ * & 0 & * \\ * & * & * \end{pmatrix}$	$\begin{pmatrix} * & * & * \\ * & * & * \\ * & * & 0 \end{pmatrix}$
Type 2	$\begin{pmatrix} 0 & * & * \\ * & * & * \\ * & * & * \end{pmatrix}$	$\begin{pmatrix} * & * & * \\ * & 0 & * \\ * & * & * \end{pmatrix}$	$\begin{pmatrix} * & * & * \\ * & * & * \\ * & * & * \end{pmatrix}$
Type 3	$\begin{pmatrix} 0 & 0 & 0 \\ 0 & * & * \\ 0 & * & * \end{pmatrix}$	$\begin{pmatrix} 0 & * & * \\ * & * & * \\ * & * & * \end{pmatrix}$	$\begin{pmatrix} 0 & * & * \\ * & * & * \\ * & * & * \end{pmatrix}$
Type 4	$\begin{pmatrix} 0 & 0 & 0 \\ 0 & * & * \\ 0 & * & * \end{pmatrix}$	$\begin{pmatrix} 0 & * & * \\ * & 0 & * \\ * & * & * \end{pmatrix}$	$\begin{pmatrix} 0 & * & * \\ * & * & * \\ * & * & * \end{pmatrix}$
Type 5	$\begin{pmatrix} 0 & * & * \\ * & * & * \\ * & * & * \end{pmatrix}$	$\begin{pmatrix} * & * & * \\ * & * & * \\ * & * & * \end{pmatrix}$	$\begin{pmatrix} * & * & * \\ * & * & * \\ * & * & * \end{pmatrix}$
Type 6	$\begin{pmatrix} * & * & * \\ * & * & * \\ * & * & * \end{pmatrix}$	$\begin{pmatrix} * & * & * \\ * & * & * \\ * & * & * \end{pmatrix}$	$\begin{pmatrix} * & * & * \\ * & * & * \\ * & * & * \end{pmatrix}$
Type 7	$\begin{pmatrix} 0 & 0 & 0 \\ 0 & 0 & * \\ 0 & * & * \end{pmatrix}$	$\begin{pmatrix} 0 & 0 & * \\ 0 & 0 & 0 \\ * & 0 & * \end{pmatrix}$	$\begin{pmatrix} 0 & * & * \\ * & 0 & * \\ * & * & * \end{pmatrix}$
Type 8	$\begin{pmatrix} 0 & 0 & 0 \\ 0 & 0 & * \\ 0 & * & * \end{pmatrix}$	$\begin{pmatrix} 0 & 0 & * \\ 0 & 0 & * \\ * & * & * \end{pmatrix}$	$\begin{pmatrix} 0 & * & * \\ * & * & * \\ * & * & * \end{pmatrix}$
Type 9	$\begin{pmatrix} 0 & 0 & 0 \\ 0 & * & * \\ 0 & * & * \end{pmatrix}$	$\begin{pmatrix} 0 & * & * \\ * & 0 & * \\ * & * & * \end{pmatrix}$	$\begin{pmatrix} 0 & * & * \\ * & * & * \\ * & * & 0 \end{pmatrix}$
Type 10	$\begin{pmatrix} 0 & 0 & 0 \\ 0 & 0 & * \\ 0 & * & * \end{pmatrix}$	$\begin{pmatrix} 0 & 0 & * \\ 0 & 0 & * \\ * & * & * \end{pmatrix}$	$\begin{pmatrix} 0 & * & * \\ * & * & * \\ * & * & 0 \end{pmatrix}$
Type 11	$\begin{pmatrix} 0 & 0 & 0 \\ 0 & 0 & * \\ 0 & * & * \end{pmatrix}$	$\begin{pmatrix} 0 & 0 & * \\ 0 & 0 & 0 \\ * & 0 & * \end{pmatrix}$	$\begin{pmatrix} 0 & * & * \\ * & 0 & * \\ * & * & 0 \end{pmatrix}$

3.2 CICYs with $h^{1,1} = 2$

In this section, we focus on CICYs with $h^{1,1} = 2$, which are reviewed in the previous section. For illustrating models, we analyze the Yukawa textures and mass hierarchies for two generations of matter fields A^a with $a = 1, 2$. We assume that either A^1 or A^2 plays the role of the Higgs field and develops a vacuum expectation value (VEV). As discussed above,

four distinct types of Yukawa textures arise in this case. To examine their phenomenological implications, we select one example from each type and analyze its mass structure in detail.

• **Type 1 (CICY 7644)**

As an illustrative example of Type 1, we examine CICY 7644. (2×2) matrices of holomorphic Yukawa couplings are obtained from the intersection numbers as

$$\kappa_{ab1} = \begin{pmatrix} 4 & 12 \\ 12 & 12 \end{pmatrix}, \quad (3.1)$$

when the Higgs field corresponds to A^1 , and

$$\kappa_{ab2} = \begin{pmatrix} 12 & 12 \\ 12 & 4 \end{pmatrix}, \quad (3.2)$$

when the Higgs field corresponds to A^2 . The ratios of the eigenvalues of both matrices are of $\mathcal{O}(1)$. However, physical Yukawa couplings can be hierarchical [86]. The Kähler metric in Eqs. (2.1) and (2.2) depends on the Kähler moduli and mixes the two generations of matter fields A^1 and A^2 . We rotate A^a ($a = 1, 2$) to $A^{\hat{a}}$, where the Kähler metric is diagonal. Then, we normalize canonically their kinetic terms. We estimate physical Yukawa couplings $Y_{\hat{a}\hat{b}1}$ and $Y_{\hat{a}\hat{b}2}$ in this basis. These physical Yukawa couplings depend on moduli. Note that we do not rotate the Higgs basis, which correspond to the original moduli basis.

Figure 1 shows the mass ratios m_1/m_2 , which are obtained from eigenvalue ratios of $Y_{\hat{a}\hat{b}1}$ and $Y_{\hat{a}\hat{b}2}$. We restrict ourselves to the region of moduli space with $\text{Re} T^a \geq 1$. As the volume increases, the mass ratio m_1/m_2 becomes smaller. The intersection numbers and holomorphic Yukawa couplings are symmetric under exchange between T^1 and T^2 . Thus, the curves in the left and right panels of Figure 1 coincide. We need $\mathcal{V} = \mathcal{O}(10^3)$ to realize $m_1/m_2 = \mathcal{O}(10^{-1})$.

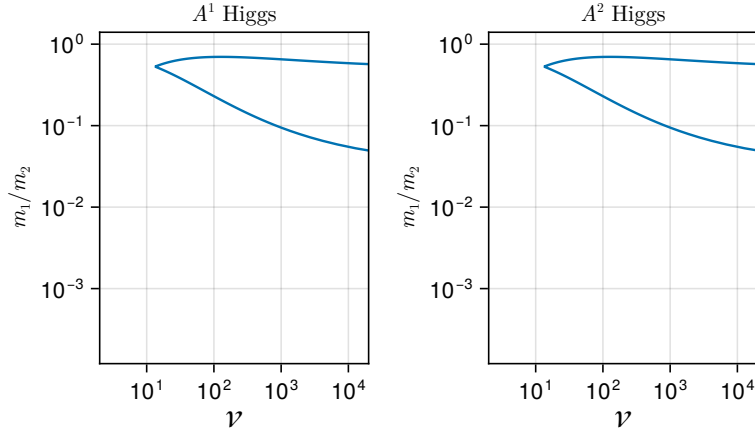


Figure 1: Mass ratios for CICY 7644 as a function of the minimum volume \mathcal{V} where all real parts of the moduli are greater than or equal to 1. The masses are ordered as $m_1 < m_2$. The left (right) panel shows the ratio m_1/m_2 for the first (second) Higgs. The lower curve in the left (right) panel corresponds to the region $\text{Re } T^1 < \text{Re } T^2$ ($\text{Re } T^1 > \text{Re } T^2$).

• **Type 2 (CICY 7643)**

As an illustrating example of Type 2, we examine CICY 7643. The holomorphic Yukawa matrices are obtained from intersection numbers as

$$\kappa_{ab1} = \begin{pmatrix} 0 & 4 \\ 4 & 12 \end{pmatrix}, \quad (3.3)$$

when the Higgs field corresponds to A^1 , and

$$\kappa_{ab2} = \begin{pmatrix} 4 & 12 \\ 12 & 8 \end{pmatrix}, \quad (3.4)$$

when the Higgs field corresponds to A^2 .

Similar to Type 1, we study physical Yukawa couplings and examine mass ratios. Figure 2 shows mass ratios m_1/m_2 depending on the volume. For $\mathcal{V} < 10^3$, the case with the Higgs field A^1 can lead to smaller ratio m_1/m_2 , while for $\mathcal{V} > 10^3$ the case with the Higgs field A^2 can lead to smaller ratio m_1/m_2 .

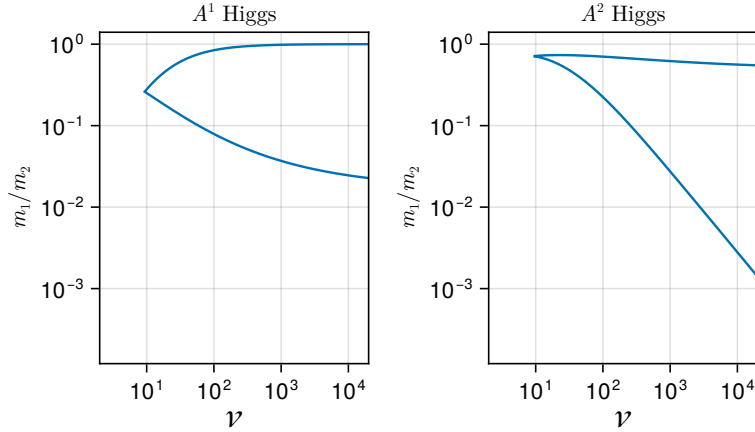


Figure 2: Mass ratios for CICY 7643 as a function of the minimum volume \mathcal{V} where all real parts of the moduli are greater than or equal to 1. The masses are ordered as $m_1 < m_2$. The left (right) panel shows the ratio m_1/m_2 for the first (second) Higgs. The lower curve in the left (right) panel corresponds to the region $\text{Re } T^1 < \text{Re } T^2$ ($\text{Re } T^1 > \text{Re } T^2$).

• **Type 3 (CICY 7806)**

As an illustrating example of Type 3, we examine CICY 7806. The holomorphic Yukawa matrices are obtained from intersection numbers as

$$\kappa_{ab1} = \begin{pmatrix} 0 & 0 \\ 0 & 6 \end{pmatrix}, \quad (3.5)$$

when the Higgs field corresponds to A^1 , and

$$\kappa_{ab2} = \begin{pmatrix} 0 & 6 \\ 6 & 6 \end{pmatrix}, \quad (3.6)$$

when the Higgs field corresponds to A^2 .

Figure 3 shows mass ratios depending on the volume. In this example, the (2×2) matrix $Y_{\hat{a}\hat{b}1}$ as well as κ_{ab1} has rank 1. Thus, we have $m_1 = 0$ for any moduli values when the Higgs field correspond to A^1 . When the Higgs field corresponds to A^2 , the mass ratio m_1/m_2 is not suppressed compared with other examples.

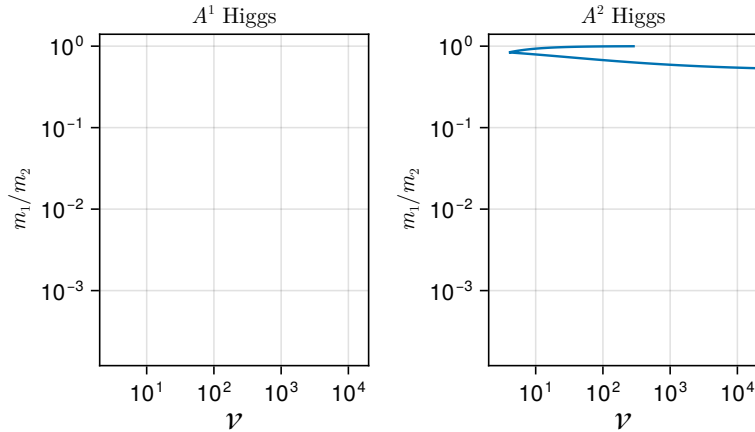


Figure 3: Mass ratios for CICY 7806 as a function of the minimum volume \mathcal{V} where all real parts of the moduli are greater than or equal to 1. The masses are ordered as $m_1 < m_2$. The left (right) panel shows the ratio m_1/m_2 for the first (second) Higgs. The lower curve in the right panel corresponds to the region $\text{Re } T^1 < \text{Re } T^2$.

• **Type 4 (CICY 7884)**

As an example of Type 4, we examine CICY 7884. The holomorphic Yukawa matrices are obtained from the intersecting numbers as

$$\kappa_{ab1} = \begin{pmatrix} 0 & 3 \\ 3 & 3 \end{pmatrix}, \quad (3.7)$$

when the Higgs field corresponds to A^1 , and

$$\kappa_{ab2} = \begin{pmatrix} 3 & 3 \\ 3 & 0 \end{pmatrix}, \quad (3.8)$$

when the Higgs field corresponds to A^2 .

Figure 4 shows mass ratios depending on the volume. The intersecting numbers and holomorphic Yukawa couplings are symmetric under exchange between T^1 and T^2 . Thus, the curves in left and right panels of Figure 4 coincide. This example leads to most suppressed mass ratio m_1/m_2 among four examples. For example, we can realize $m_1/m_2 = \mathcal{O}(10^{-2})$ for $V = \mathcal{O}(10^{2.5})$.

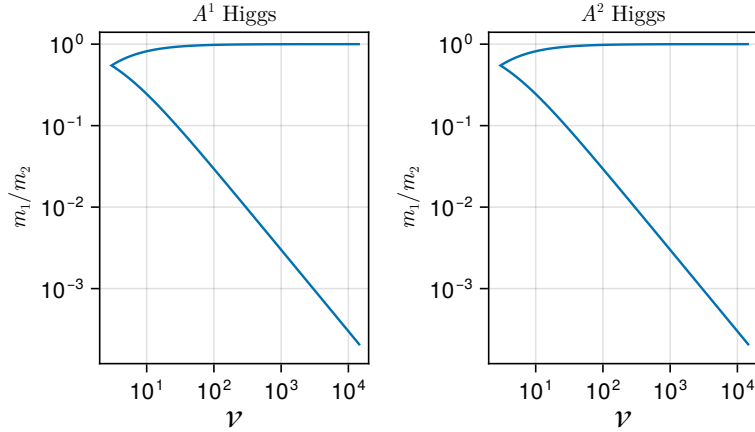


Figure 4: Mass ratios for CICY 7884 as a function of the minimum volume \mathcal{V} where all real parts of the moduli are greater than or equal to 1. The masses are ordered as $m_1 < m_2$. The left (right) panel shows the ratio m_1/m_2 for the first (second) Higgs. The lower curve in the left (right) panel corresponds to the region $\text{Re } T^1 < \text{Re } T^2$ ($\text{Re } T^1 > \text{Re } T^2$).

3.3 CICYs with $h^{1,1} = 3$

Similar to the previous section, here we study Yukawa textures and mass ratios for CICYs with $h^{1,1} = 3$. There are three generations of matter fields A^a with $a = 1, 2, 3$. We assume that one of the A^a ($a = 1, 2, 3$) plays the role of the Higgs field and develops its VEV. In this case, eleven distinct types arise. To investigate their phenomenological aspects, we select one representative example from each type and analyze it in detail. In particular, we present three types, namely Type 1, Type 6 and Type 10. The other cases are shown in Appendix A.

• Type 1 (CICY 5299)

As an illustrative example of Type 1, we examine CICY 5299. The holomorphic Yukawa matrices are obtained from the intersection numbers as

$$\kappa_{ab1} = \begin{pmatrix} 0 & 2 & 4 \\ 2 & 4 & 9 \\ 4 & 9 & 2 \end{pmatrix}, \quad (3.9)$$

when the Higgs field corresponds to A^1 ,

$$\kappa_{ab2} = \begin{pmatrix} 2 & 4 & 9 \\ 4 & 0 & 2 \\ 9 & 2 & 4 \end{pmatrix}, \quad (3.10)$$

when the Higgs field corresponds to A^2 , and

$$\kappa_{ab3} = \begin{pmatrix} 4 & 9 & 2 \\ 9 & 2 & 4 \\ 2 & 4 & 0 \end{pmatrix}, \quad (3.11)$$

when the Higgs field corresponds to A^3 .

Figure 5 shows the mass ratios m_1/m_3 and m_2/m_3 , which are obtained from eigenvalue ratios of $Y_{\hat{a}\hat{b}1}$, $Y_{\hat{a}\hat{b}2}$ and $Y_{\hat{a}\hat{b}3}$. The points correspond to discrete variations of the moduli ratio $T^1 : T^2 : T^3$, subject to the restriction $\text{Re} T^a \geq 1$.

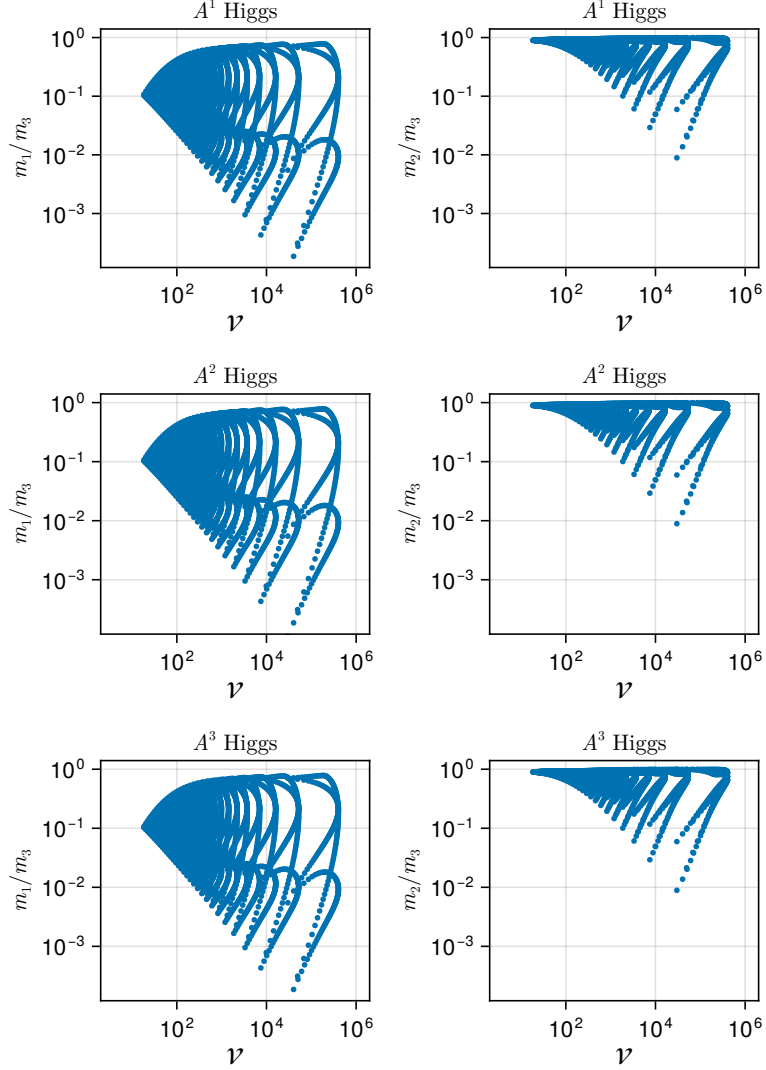


Figure 5: Mass ratios for CICY 5299 as a function of the minimum volume \mathcal{V} where all real parts of the moduli are greater than or equal to 1. The masses are ordered as $m_1 < m_2 < m_3$. The left (right) panel shows the scatter for m_1/m_3 (m_2/m_3).

- **Type 6 (CICY 7242)**

As an illustrative example of Type 6, we examine CICY 7242. The holomorphic Yukawa

matrices are obtained from the intersection numbers as

$$\kappa_{ab1} = \begin{pmatrix} 2 & 6 & 6 \\ 6 & 6 & 10 \\ 6 & 10 & 6 \end{pmatrix}, \quad (3.12)$$

when the Higgs field corresponds to A^1 ,

$$\kappa_{ab2} = \begin{pmatrix} 6 & 6 & 10 \\ 6 & 2 & 6 \\ 10 & 6 & 6 \end{pmatrix}, \quad (3.13)$$

when the Higgs field corresponds to A^2 , and

$$\kappa_{ab3} = \begin{pmatrix} 6 & 10 & 6 \\ 10 & 6 & 6 \\ 6 & 6 & 2 \end{pmatrix}, \quad (3.14)$$

when the Higgs field corresponds to A^3 .

Figure 6 shows the mass ratios m_1/m_3 and m_2/m_3 , which are obtained from eigenvalue ratios of $Y_{\hat{a}\hat{b}1}$, $Y_{\hat{a}\hat{b}2}$ and $Y_{\hat{a}\hat{b}3}$. The points correspond to discrete variations of the moduli ratio $T^1 : T^2 : T^3$, subject to the restriction $\text{Re} T^a \geq 1$.

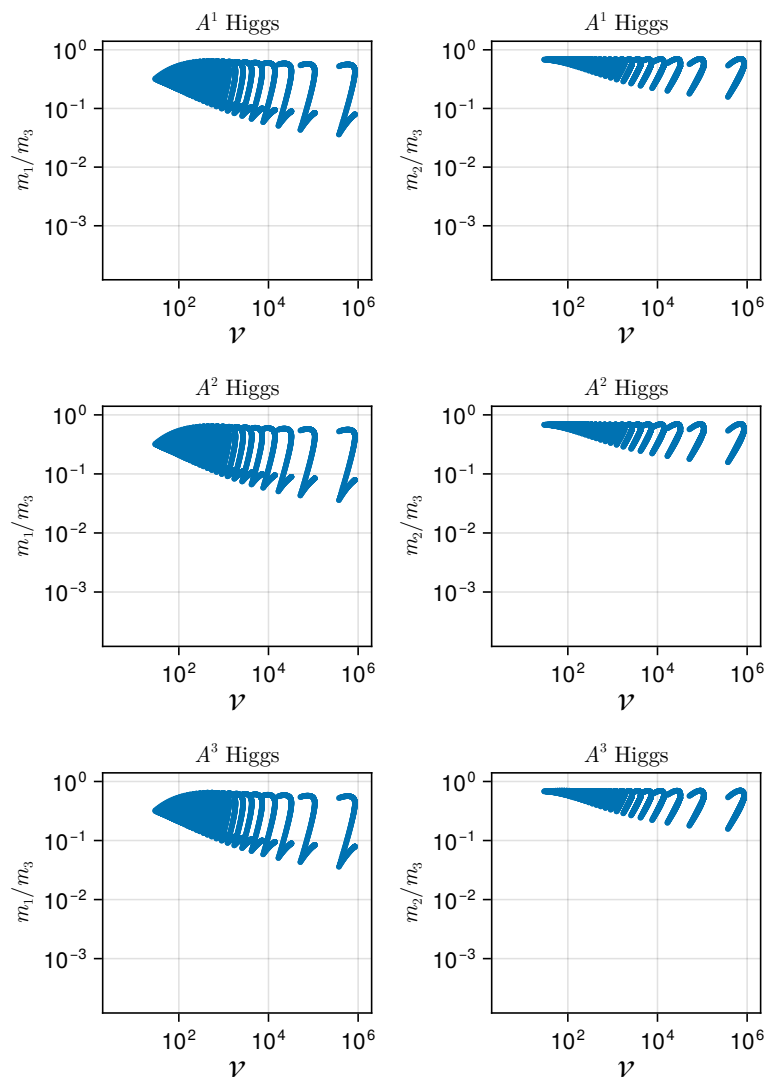


Figure 6: Mass ratios for CICY 7242 as a function of the minimum volume \mathcal{V} where all real parts of the moduli are greater than or equal to 1. The masses are ordered as $m_1 < m_2 < m_3$. The left (right) panel shows the scatter for m_1/m_3 (m_2/m_3).

- **Type 10 (CICY 7875)**

As an illustrative example of Type 10, we examine CICY 7875. The holomorphic Yukawa matrices are obtained from the intersection numbers as

$$\kappa_{ab1} = \begin{pmatrix} 0 & 0 & 0 \\ 0 & 0 & 3 \\ 0 & 3 & 2 \end{pmatrix}, \quad (3.15)$$

when the Higgs field corresponds to A^1 ,

$$\kappa_{ab2} = \begin{pmatrix} 0 & 0 & 3 \\ 0 & 0 & 3 \\ 3 & 3 & 3 \end{pmatrix}, \quad (3.16)$$

when the Higgs field corresponds to A^2 , and

$$\kappa_{ab3} = \begin{pmatrix} 0 & 3 & 2 \\ 3 & 3 & 3 \\ 2 & 3 & 0 \end{pmatrix}, \quad (3.17)$$

when the Higgs field corresponds to A^3 .

Figure 7 shows the mass ratios m_1/m_3 and m_2/m_3 , which are obtained from eigenvalue ratios of $Y_{\hat{a}\hat{b}1}$, $Y_{\hat{a}\hat{b}2}$ and $Y_{\hat{a}\hat{b}3}$. The points correspond to discrete variations of the moduli ratio $T^1 : T^2 : T^3$, subject to the restriction $\text{Re}T^a \geq 1$. In this example, the (3×3) matrices $Y_{\hat{a}\hat{b}1}$ and $Y_{\hat{a}\hat{b}2}$ have rank 2. When the Higgs field corresponds to A^1 and A^2 , we have $m_1 = 0$ for any moduli values.

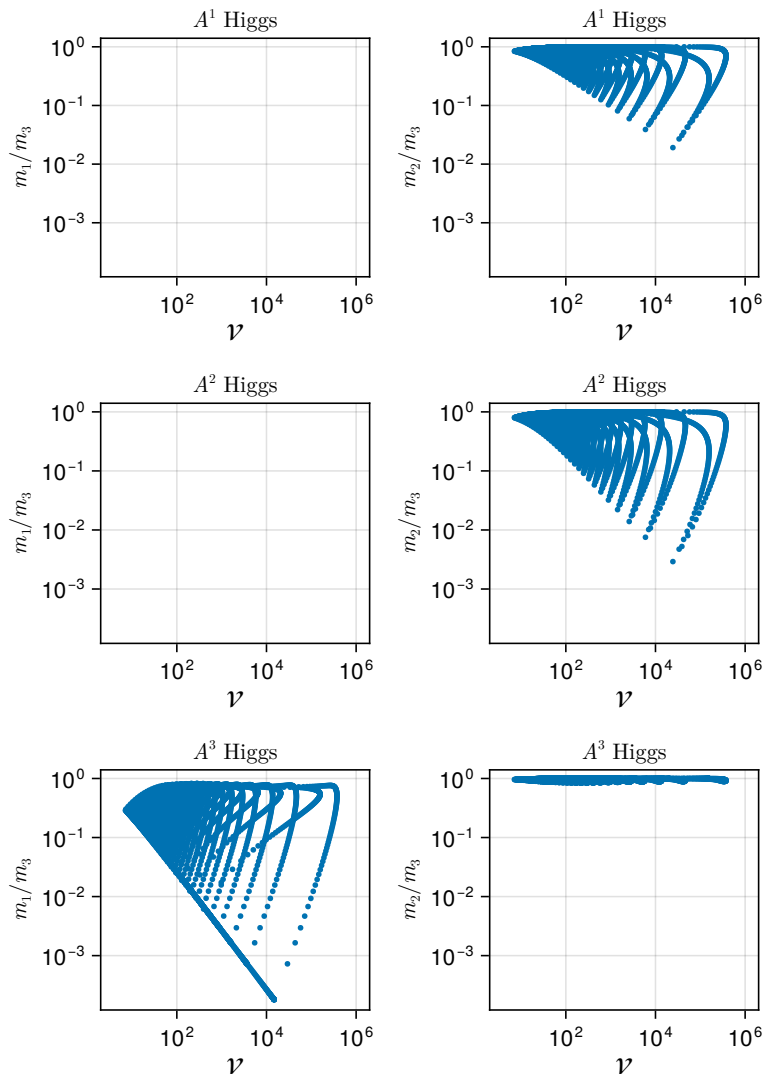


Figure 7: Mass ratios for CICY 7875 as a function of the minimum volume \mathcal{V} where all real parts of the moduli are greater than or equal to 1. The masses are ordered as $m_1 < m_2 < m_3$. The left (right) panel shows the scatter for m_1/m_3 (m_2/m_3).

3.4 Phenomenological implications

The results for CICYs with $h^{1,1} = 3$ in the previous section show that mass hierarchies, in particular small values of m_1/m_3 , can be realized when the volume \mathcal{V} is large. For $\mathcal{V} = 10^2$, we obtain $m_1/m_3 = 10^{-1} - 10^{-2}$. For $\mathcal{V} = 10^3$, even smaller values such as $m_1/m_3 = 10^{-3}$ or below can be achieved.

Quark and lepton mass ratios are estimated e.g. at 10^{16} GeV as [87]

$$\begin{aligned} \frac{m_c}{m_t} &\sim 3 \times 10^{-3}, & \frac{m_u}{m_t} &\sim 6 \times 10^{-6}, \\ \frac{m_s}{m_b} &\sim 2 \times 10^{-2}, & \frac{m_d}{m_b} &\sim 1 \times 10^{-3}, \\ \frac{m_\mu}{m_\tau} &\sim 6 \times 10^{-2}, & \frac{m_e}{m_\tau} &\sim 3 \times 10^{-4}. \end{aligned} \quad (3.18)$$

In order to realize these large mass hierarchies, we need a large CY volume \mathcal{V} . However, \mathcal{V} is related to the four-dimensional gauge coupling via Eq. (2.4). The gauge coupling at the GUT scale is estimated as $\alpha^{-1}(M_{\text{GUT}}) \simeq 25$ with $M_{\text{GUT}} \simeq 2 \times 10^{16}$ GeV in the minimal supersymmetric Standard Model, while we estimate as $\alpha^{-1}(M_{\text{GUT}}) \sim 50$ in the Standard Model. Requiring the weak string coupling $g_s \leq 1$ leads to the constraint on the volume as $\mathcal{V} \lesssim 25$ or 50 , depending on the running coupling behavior. Under this constraint, we may realize smaller hierarchy like $m_1/m_3 \gtrsim 10^{-1} - 10^{-2}$ from the results in the previous section. If additional effects from lighter gauge bosons are present,⁴ we may obtain larger value of $\alpha^{-1}(M_{\text{GUT}})$, allowing for larger \mathcal{V} .

So far, we have assumed that the (light) Higgs field, which develops its VEV, corresponds to one of the A^a in the original moduli basis. However, the light Higgs direction may correspond to the mixed direction of the original moduli basis, $\sum_a c_a A^a$ in general. Indeed, generic string compactifications typically contain many candidates for the Higgs fields. That is the multi-Higgs models at the compactification scale. The light Higgs field would be determined by their mass terms, which may be generated by VEVs of other fields and/or non-perturbative effects. The precise structure depends on the details of mass generation mechanism. Such a discussion on mass generation scenarios is beyond our scope. Here we parametrize the light Higgs direction and demonstrate interesting results.

Suppose that the light Higgs direction, which develop its VEV, is given by $A^1 + \varepsilon A^3$ in the CICY 7806 model of type 3 with $h^{1,1} = 2$. Then the holomorphic (2×2) Yukawa matrix takes the form:

$$\kappa_{ab} \sim 6 \begin{pmatrix} 0 & \varepsilon \\ \varepsilon & 1 \end{pmatrix}. \quad (3.19)$$

This structure leads to a mass hierarchy as well as a mixing angle controlled by ε , similar to the down sector of the Weinberg texture [85].

Similarly, suppose that the light Higgs direction, which develops its VEV, is written by $A^1 + \varepsilon A^3$ in CICY 7465 of type 10 with $h^{1,1} = 3$. We set $\varepsilon = 0.1, 0.01, 0.001$. Figure 8 shows the mass ratios. The mass ratio m_1/m_3 can be small depending on ε , even for $\mathcal{V} \lesssim 50$. Note that the mass matrix has rank 2 along the A^1 direction, while the mass matrix has rank 3 along the A^3 direction. This interplay leads to the hierarchical structure. Also, we can find the direction leading to the rank-2 mass matrix in other CICY models with $h^{1,1} = 3$. However, we can not find rank-1 (3×3) mass matrices in CICY models with $h^{1,1} = 3$.

⁴The correction $\Delta\alpha^{-1}$ is estimated as $\Delta\alpha^{-1} = b \ln M_{\text{GUT}}/M_V$, where b is the one-loop beta function coefficient and M_V denotes a vector boson mass lighter than M_{GUT} .

We extend the above analysis to CICY models with $h^{1,1} = 4$. Their coupling selection rules are classified in Ref. [74]. We use CICY 5245 as an example. We assume that three A^1, A^2 , and A^4 among four A^a correspond to three generations. Then, the (3×3) mass matrix becomes rank-1, i.e., $m_1 = m_2 = 0$ if the light Higgs direction, which develops its VEV, corresponds to

$$A^0 = 3A^1 + 6A^2 - 4A^3 + 2A^4. \quad (3.20)$$

A small deviation from this direction may generate large hierarchies among m_1, m_2 and m_3 . For example, we consider the deviation like $A^0 + \varepsilon_1 A^1 + \varepsilon_3 A^3$. Figures 9, 10 and 11 show the mass ratios m_1/m_3 and m_2/m_3 when $(\varepsilon_1, \varepsilon_3) = (0.2, 0.001)$, $(0.4, 0.05)$, and $(0.9, 0.09)$. In the limit that $\varepsilon_1, \varepsilon_3 \rightarrow 0$, two mass eigenvalues m_1 and m_2 vanish and a $U(2)$ flavor symmetry emerges. Such $U(2)$ flavor symmetry and its small violation are phenomenologically interesting in particle physics, e.g., in controlling flavor-dependent operators in the Standard Model effective field theory [88–91]. This scenario provides us with a concrete realization of $U(2)$ flavor symmetry scenario. Furthermore, higher-dimensional operators are also governed by the prepotential of moduli fields [92], and this observation supports the hypothesis of minimal flavor violation in string-derived low energy effective field theory [93].⁵

⁵See also Refs. [94–96].

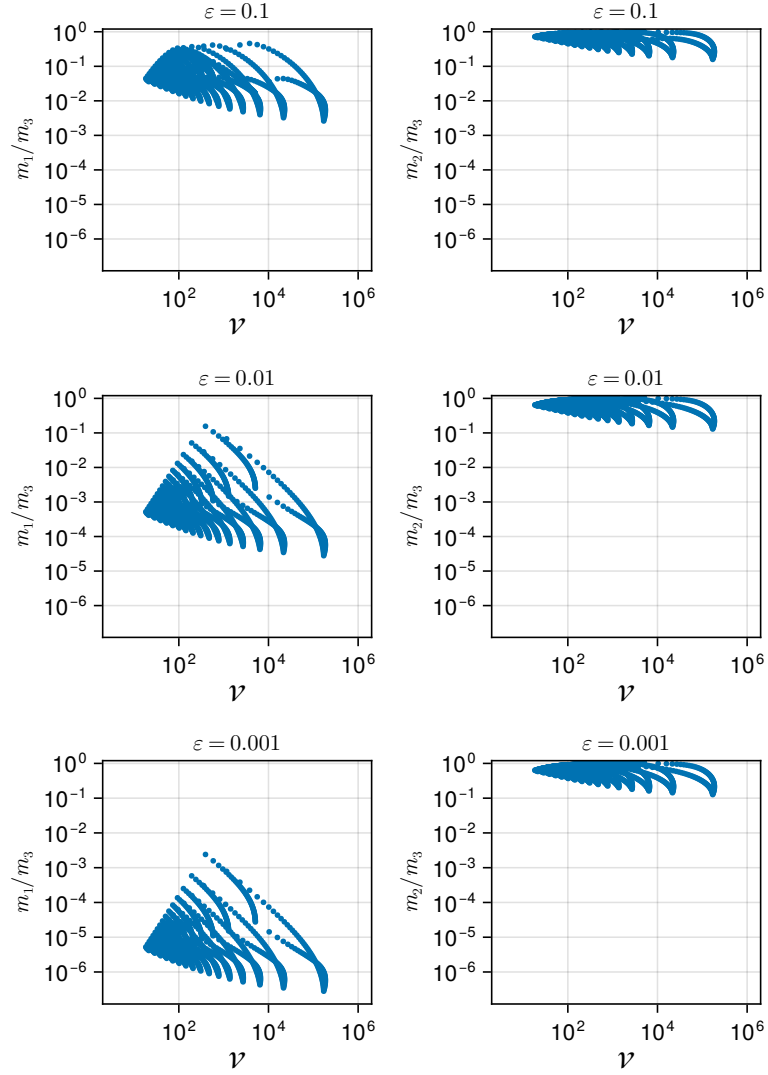


Figure 8: Mass ratios for CICY 7465 as a function of the minimum volume \mathcal{V} when the Higgs field is assigned to $A^1 + \varepsilon A^3$ ($\varepsilon = 0.1, 0.01, 0.001$), where all real parts of the moduli are greater than or equal to 1. The masses are ordered as $m_1 < m_2 < m_3$. The left (right) panel shows the scatter for m_1/m_3 (m_2/m_3).

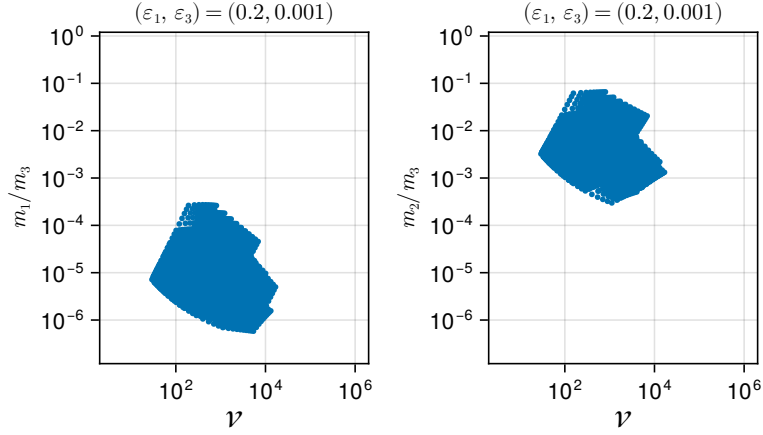


Figure 9: Mass ratios for CICY 5245 as a function of the minimum volume \mathcal{V} when the Higgs field is assigned to $A^0 + 0.2 \cdot A^1 + 0.001 \cdot A^3$ ($A^0 = 3A^1 + 6A^2 - 4A^3 + 2A^4$), where all real parts of the moduli are greater than or equal to 1. The three fermion generations are assigned to A^1, A^2, A^4 . The masses are ordered as $m_1 < m_2 < m_3$. The left (right) panel shows the scatter for m_1/m_3 (m_2/m_3).

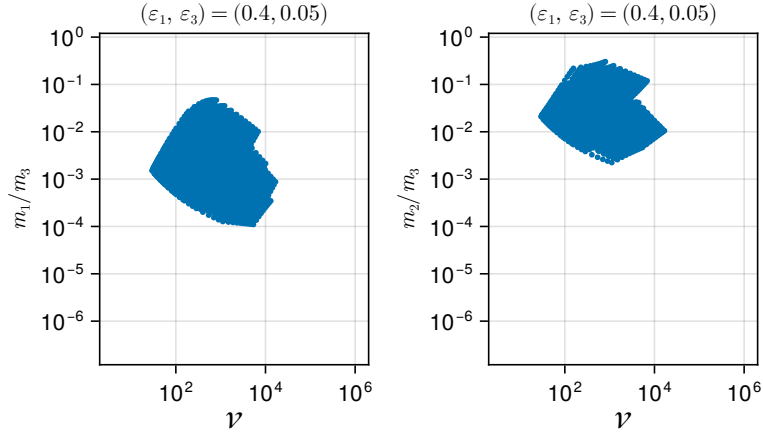


Figure 10: Mass ratios for CICY 5245 as a function of the minimum volume \mathcal{V} when the Higgs field is assigned to $A^0 + 0.4 \cdot A^1 + 0.05 \cdot A^3$ ($A^0 = 3A^1 + 6A^2 - 4A^3 + 2A^4$), where all real parts of the moduli are greater than or equal to 1. The three fermion generations are assigned to A^1, A^2, A^4 . The masses are ordered as $m_1 < m_2 < m_3$. The left (right) panel shows the scatter for m_1/m_3 (m_2/m_3).

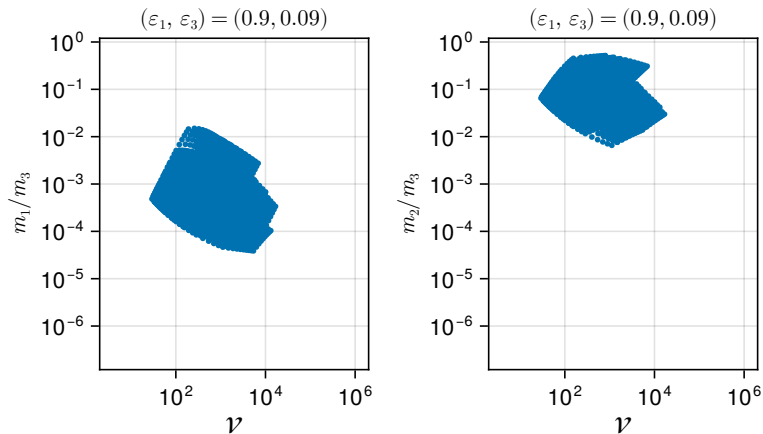


Figure 11: Mass ratios for CICY 5245 as a function of the minimum volume \mathcal{V} when the Higgs field is assigned to $A^0 + 0.9 \cdot A^1 + 0.09 \cdot A^3$ ($A^0 = 3A^1 + 6A^2 - 4A^3 + 2A^4$), where all real parts of the moduli are greater than or equal to 1. The three fermion generations are assigned to A^1, A^2, A^4 . The masses are ordered as $m_1 < m_2 < m_3$. The left (right) panel shows the scatter for m_1/m_3 (m_2/m_3).

Moreover, let us assume that the light Higgs directions in the up-sector and down-sector are different from each other, analogous to the minimal supersymmetric Standard Model: $A^0 + \varepsilon_{u1}A^1 + \varepsilon_{u3}A^3$ for the up-sector and $A^0 + \varepsilon_{d1}A^1 + \varepsilon_{d3}A^3$ for the down-sector. Table 7 shows representative examples of mass ratios and mixing angles, derived from specific values of the moduli T^a and parameters $\varepsilon_{u1}, \varepsilon_{u3}, \varepsilon_{d1}, \varepsilon_{d3}$. They realize the orders of experimental values, although we do not fully reproduce all of experimental data for mass hierarchies and mixing angles. Hence, this direction to study is interesting and has a potential to realize experimental data. We would study more systematically other CICY models elsewhere.

As emphasized above, Yukawa textures, in particular rank-reduced matrices and small perturbations around them, play a crucial role in these types of models.⁶ At any rate, the light Higgs direction is determined by the mass matrix of Higgs fields. If they depend on moduli, we may need fine-tuning to realize the hierarchical structures discussed above. One of the interesting possibilities is that moduli are trapped dynamically at special points where additional massless modes appear [98, 99]. In such a scenario, the moduli may be trapped around the point, where the rank of the mass matrix is reduced, although we need a certain mechanism to stabilize moduli around the point with an enhanced symmetry.

⁶See Ref. [97] for a similar scenario in magnetized orbifold models.

Table 7: Mass ratios and mixing angles.

(T^1, T^2, T^3, T^4)	ν	$\begin{pmatrix} \varepsilon_{u1} \\ \varepsilon_{u3} \end{pmatrix}$	$\begin{pmatrix} \varepsilon_{d1} \\ \varepsilon_{d3} \end{pmatrix}$	$\begin{pmatrix} m_u/m_t \\ m_c/m_t \\ m_d/m_b \\ m_s/m_b \end{pmatrix}$	$\begin{pmatrix} V_{us} \\ V_{cb} \\ V_{ub} \end{pmatrix}$
$(1, 4, 1, 1)$	71	$\begin{pmatrix} 0.10 \\ 3.2 \times 10^{-4} \end{pmatrix}$	$\begin{pmatrix} 0.18 \\ 7.9 \times 10^{-3} \end{pmatrix}$	$\begin{pmatrix} 5 \times 10^{-6} \\ 4 \times 10^{-3} \\ 6 \times 10^{-4} \\ 2 \times 10^{-2} \end{pmatrix}$	$\begin{pmatrix} 0.20 \\ 0.052 \\ 0.006 \end{pmatrix}$
$(1, 3, 1, 1)$	57	$\begin{pmatrix} 0.11 \\ 3.2 \times 10^{-4} \end{pmatrix}$	$\begin{pmatrix} 0.18 \\ 7.9 \times 10^{-3} \end{pmatrix}$	$\begin{pmatrix} 4 \times 10^{-6} \\ 3 \times 10^{-3} \\ 6 \times 10^{-4} \\ 1 \times 10^{-2} \end{pmatrix}$	$\begin{pmatrix} 0.20 \\ 0.037 \\ 0.005 \end{pmatrix}$
$(1, 1.25, 1, 1)$	33	$\begin{pmatrix} 0.16 \\ 5.0 \times 10^{-4} \end{pmatrix}$	$\begin{pmatrix} 0.28 \\ 0.016 \end{pmatrix}$	$\begin{pmatrix} 3 \times 10^{-6} \\ 3 \times 10^{-3} \\ 6 \times 10^{-4} \\ 1 \times 10^{-2} \end{pmatrix}$	$\begin{pmatrix} 0.20 \\ 0.038 \\ 0.008 \end{pmatrix}$
$(1.25, 1.25, 1, 1)$	38	$\begin{pmatrix} 0.18 \\ 1.0 \times 10^{-4} \end{pmatrix}$	$\begin{pmatrix} 0.28 \\ 0.013 \end{pmatrix}$	$\begin{pmatrix} 1 \times 10^{-7} \\ 3 \times 10^{-3} \\ 6 \times 10^{-4} \\ 1 \times 10^{-2} \end{pmatrix}$	$\begin{pmatrix} 0.23 \\ 0.032 \\ 0.006 \end{pmatrix}$
$(1, 1, 1, 1)$	29	$\begin{pmatrix} 0.22 \\ 0.010 \end{pmatrix}$	$\begin{pmatrix} 0.11 \\ 0.040 \end{pmatrix}$	$\begin{pmatrix} 4 \times 10^{-4} \\ 5 \times 10^{-3} \\ 4 \times 10^{-3} \\ 1 \times 10^{-2} \end{pmatrix}$	$\begin{pmatrix} 0.30 \\ 0.027 \\ 0.006 \end{pmatrix}$

4 Conclusions

In this paper, we have clarified the Yukawa textures of matter fields corresponding to moduli fields in the context of heterotic string theory on CY threefolds with standard embedding. In particular, we focused on CICYs with a small number of moduli. Since the selection rules for matter fields are governed by those of the moduli fields, the topological structure of the CY threefold leads to novel Yukawa structures that cannot be obtained from group-theoretical symmetries.

By analyzing the Yukawa textures of matter fields on CICYs with $h^{1,1} = 2$ in section 3.2 and $h^{1,1} = 3$ in section 3.3, we found that hierarchical structures cannot be realized in the moduli basis. This is because the CY volume is related to the magnitude of four-dimensional gauge coupling at the compactification scale, preventing us from taking the large volume regime. To overcome this problem, we analyzed a more generic region of the moduli space of multi-Higgs fields, including the Standard Model Higgs field as the lightest mode. Remarkably, in the case of CICYs with $h^{1,1} = 2$, we can realize the so-called Weinberg texture, which successfully reproduces the Cabibbo angle by the mass

ratio between the down and strange quarks. Furthermore, when the Higgs field in the Standard Model is aligned with special loci in the moduli space, the rank of the fermion mass matrix is reduced to two for CICYs with $h^{1,1} = 3$ and to one for certain CICYs with $h^{1,1} = 4$. Hence, in the rank-1 case realized in some CICYs with $h^{1,1} = 4$, a $U(2)$ flavor symmetry emerges at these special loci in the moduli space of multi-Higgs fields. It is well known that such a $U(2)$ flavor symmetry plays an important role in controlling higher-dimensional operators in the Standard Model effective field theory. Our results provide a string-theoretic framework that supports this scenario within string-derived low energy effective field theory.

When we consider small perturbations around the symmetry-enhanced loci, it is expected to generate hierarchical fermion masses. Indeed, our numerical analysis shows that CY volumes consistent with phenomenologically viable gauge couplings can reproduce the observed masses and mixing angles in the quark sector. It would be fascinating to figure out the stabilization mechanism of the Higgs fields as well as moduli fields that leads to realistic patterns of fermion masses and mixings. We will leave this important issue for future work.

Acknowledgments

This work was supported by JSPS KAKENHI Grant Numbers JP23K03375 (T.K.) and JP25H01539 (H.O.).

A $h^{1,1} = 3$

In this section, we summarize the Yukawa textures of matter fields on CICYs except for Type 1, Type 6 and Type 10.

• Type 2 (CICY 6220)

As an illustrative example of Type 2, we examine CICY 6220. The holomorphic Yukawa matrices are obtained from the intersection numbers as

$$\kappa_{ab1} = \begin{pmatrix} 0 & 3 & 2 \\ 3 & 3 & 9 \\ 2 & 9 & 6 \end{pmatrix}, \quad (\text{A.1})$$

when the Higgs field corresponds to A^1 ,

$$\kappa_{ab2} = \begin{pmatrix} 3 & 3 & 9 \\ 3 & 0 & 2 \\ 9 & 2 & 6 \end{pmatrix}, \quad (\text{A.2})$$

when the Higgs field corresponds to A^2 , and

$$\kappa_{ab3} = \begin{pmatrix} 2 & 9 & 6 \\ 9 & 2 & 6 \\ 6 & 6 & 4 \end{pmatrix}, \quad (\text{A.3})$$

when the Higgs field corresponds to A^3 .

Figure 12 shows the mass ratios m_1/m_3 and m_2/m_3 , which are obtained from eigenvalue ratios of $Y_{\hat{a}\hat{b}1}$, $Y_{\hat{a}\hat{b}2}$ and $Y_{\hat{a}\hat{b}3}$. The points correspond to discrete variations of the moduli ratio $T^1 : T^2 : T^3$, subject to the restriction $\text{Re} T^a \geq 1$.

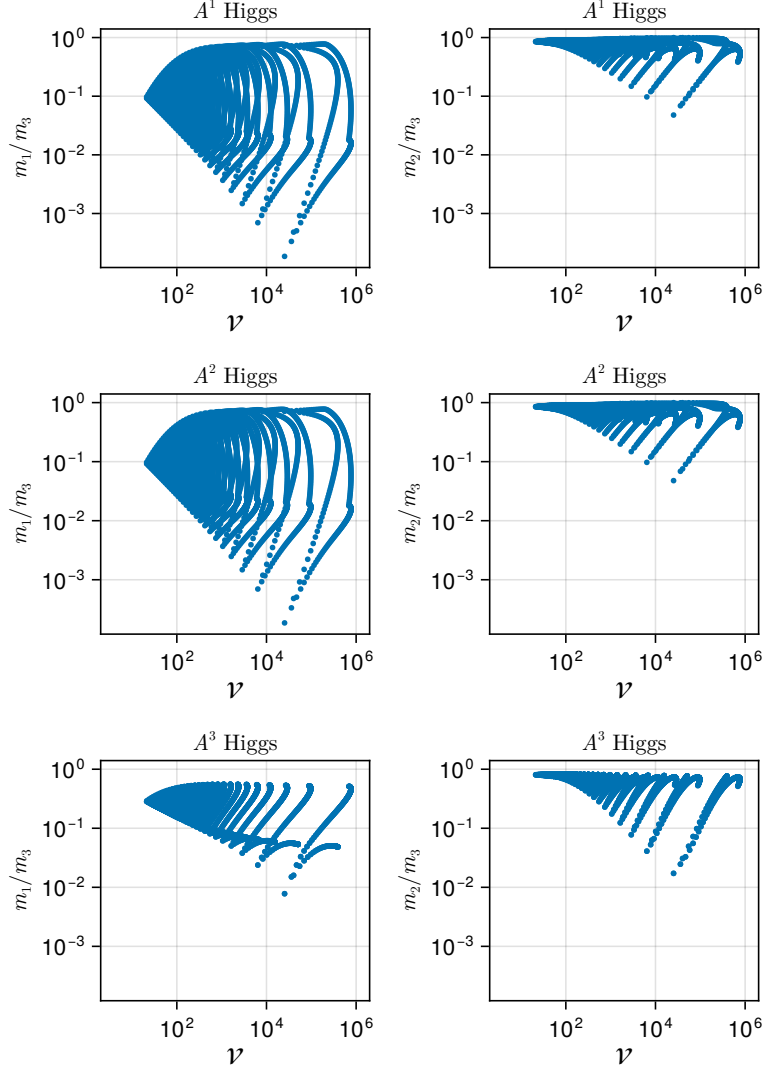


Figure 12: Mass ratios for CICY 6220 as a function of the minimum volume \mathcal{V} where all real parts of the moduli are greater than or equal to 1. The masses are ordered as $m_1 < m_2 < m_3$. The left (right) panel shows the scatter for m_1/m_3 (m_2/m_3).

- **Type 3 (CICY 6771)**

As an illustrative example of Type 3, we examine CICY 6771. The holomorphic Yukawa

matrices are obtained from the intersection numbers as

$$\kappa_{ab1} = \begin{pmatrix} 0 & 0 & 0 \\ 0 & 4 & 8 \\ 0 & 8 & 4 \end{pmatrix}, \quad (\text{A.4})$$

when the Higgs field corresponds to A^1 ,

$$\kappa_{ab2} = \begin{pmatrix} 0 & 4 & 8 \\ 4 & 2 & 6 \\ 8 & 6 & 6 \end{pmatrix}, \quad (\text{A.5})$$

when the Higgs field corresponds to A^2 , and

$$\kappa_{ab3} = \begin{pmatrix} 0 & 8 & 4 \\ 8 & 6 & 6 \\ 4 & 6 & 2 \end{pmatrix}, \quad (\text{A.6})$$

when the Higgs field corresponds to A^3 .

Figure 13 shows the mass ratios m_1/m_3 and m_2/m_3 , which are obtained from eigenvalue ratios of $Y_{\hat{a}\hat{b}1}$, $Y_{\hat{a}\hat{b}2}$ and $Y_{\hat{a}\hat{b}3}$. The points correspond to discrete variations of the moduli ratio $T^1 : T^2 : T^3$, subject to the restriction $\text{Re}T^a \geq 1$. In this example, the (3×3) matrix $Y_{\hat{a}\hat{b}1}$ has rank 1. Thus, we have $m_1 = 0$ for any moduli values when the Higgs field corresponds to A^1 .

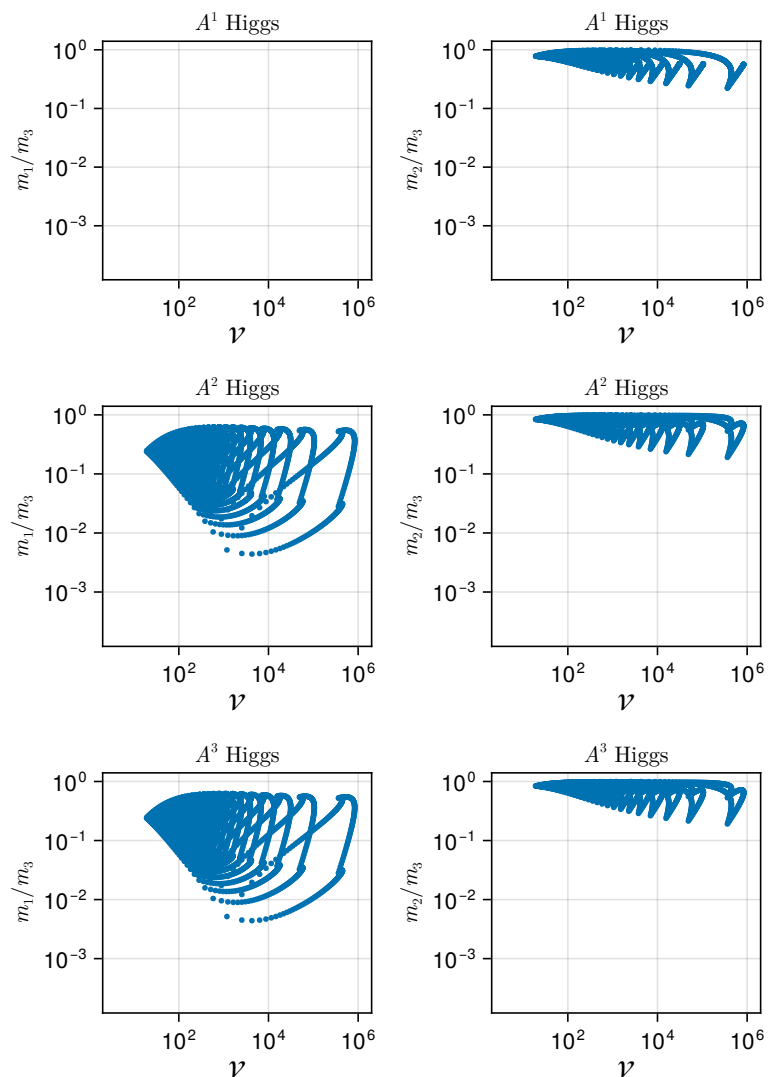


Figure 13: Mass ratios for CICY 6771 as a function of the minimum volume \mathcal{V} where all real parts of the moduli are greater than or equal to 1. The masses are ordered as $m_1 < m_2 < m_3$. The left (right) panel shows the scatter for m_1/m_3 (m_2/m_3).

- **Type 4 (CICY 7069)**

As an illustrative example of Type 4, we examine CICY 7069. The holomorphic Yukawa matrices are obtained from the intersection numbers as

$$\kappa_{ab1} = \begin{pmatrix} 0 & 0 & 0 \\ 0 & 2 & 6 \\ 0 & 6 & 4 \end{pmatrix}, \quad (\text{A.7})$$

when the Higgs field corresponds to A^1 ,

$$\kappa_{ab2} = \begin{pmatrix} 0 & 2 & 6 \\ 2 & 0 & 2 \\ 6 & 2 & 6 \end{pmatrix}, \quad (\text{A.8})$$

when the Higgs field corresponds to A^2 , and

$$\kappa_{ab3} = \begin{pmatrix} 0 & 6 & 4 \\ 6 & 2 & 6 \\ 4 & 6 & 4 \end{pmatrix}, \quad (\text{A.9})$$

when the Higgs field corresponds to A^3 .

Figure 14 shows the mass ratios m_1/m_3 and m_2/m_3 , which are obtained from eigenvalue ratios of $Y_{\hat{a}\hat{b}1}$, $Y_{\hat{a}\hat{b}2}$ and $Y_{\hat{a}\hat{b}3}$. The points correspond to discrete variations of the moduli ratio $T^1 : T^2 : T^3$, subject to the restriction $\text{Re } T^a \geq 1$. In this example, the (3×3) matrix $Y_{\hat{a}\hat{b}1}$ has rank 1. When the Higgs field corresponds to A^1 , we have $m_1 = 0$ for any moduli values.

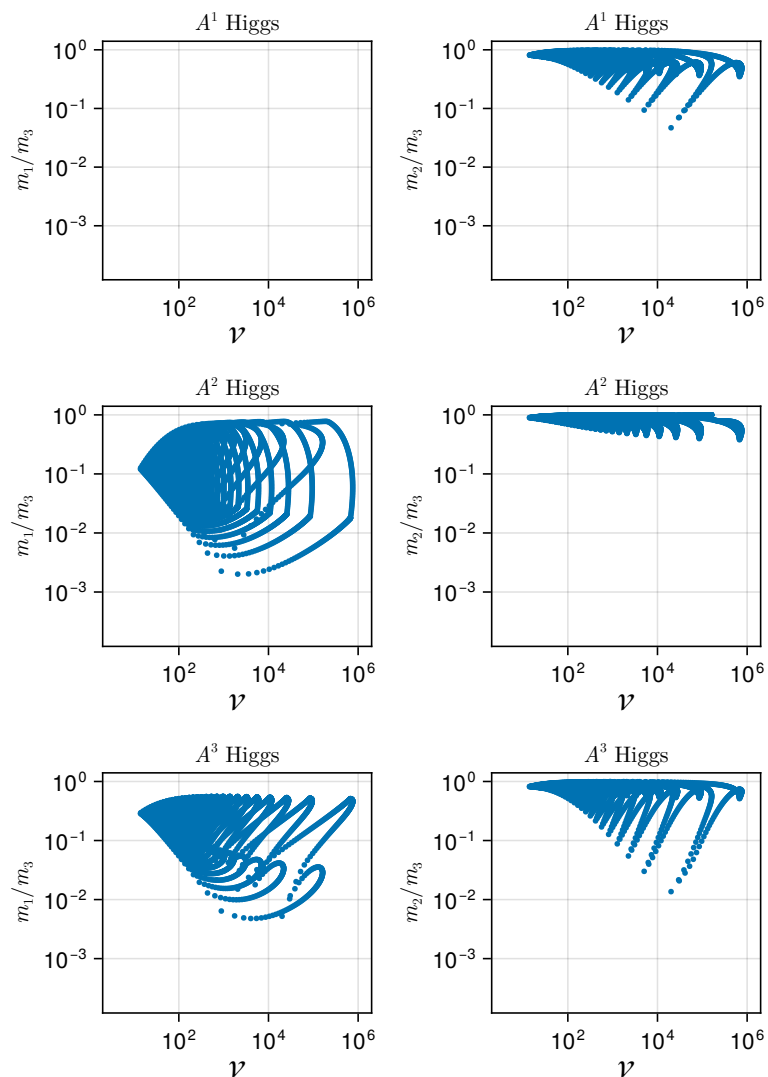


Figure 14: Mass ratios for CICY 7069 as a function of the minimum volume \mathcal{V} where all real parts of the moduli are greater than or equal to 1. The masses are ordered as $m_1 < m_2 < m_3$. The left (right) panel shows the scatter for m_1/m_3 (m_2/m_3).

- **Type 5 (CICY 7071)**

As an illustrative example of Type 5, we examine CICY 7071. The holomorphic Yukawa matrices are obtained from the intersection numbers as

$$\kappa_{ab1} = \begin{pmatrix} 0 & 2 & 4 \\ 2 & 4 & 10 \\ 4 & 10 & 8 \end{pmatrix}, \quad (\text{A.10})$$

when the Higgs field corresponds to A^1 ,

$$\kappa_{ab2} = \begin{pmatrix} 2 & 4 & 10 \\ 4 & 2 & 8 \\ 10 & 8 & 10 \end{pmatrix}, \quad (\text{A.11})$$

when the Higgs field corresponds to A^2 , and

$$\kappa_{ab3} = \begin{pmatrix} 4 & 10 & 8 \\ 10 & 8 & 10 \\ 8 & 10 & 4 \end{pmatrix}, \quad (\text{A.12})$$

when the Higgs field corresponds to A^3 .

Figure 15 shows the mass ratios m_1/m_3 and m_2/m_3 , which are obtained from eigenvalue ratios of $Y_{\hat{a}\hat{b}1}$, $Y_{\hat{a}\hat{b}2}$ and $Y_{\hat{a}\hat{b}3}$. The points correspond to discrete variations of the moduli ratio $T^1 : T^2 : T^3$, subject to the restriction $\text{Re } T^a \geq 1$.

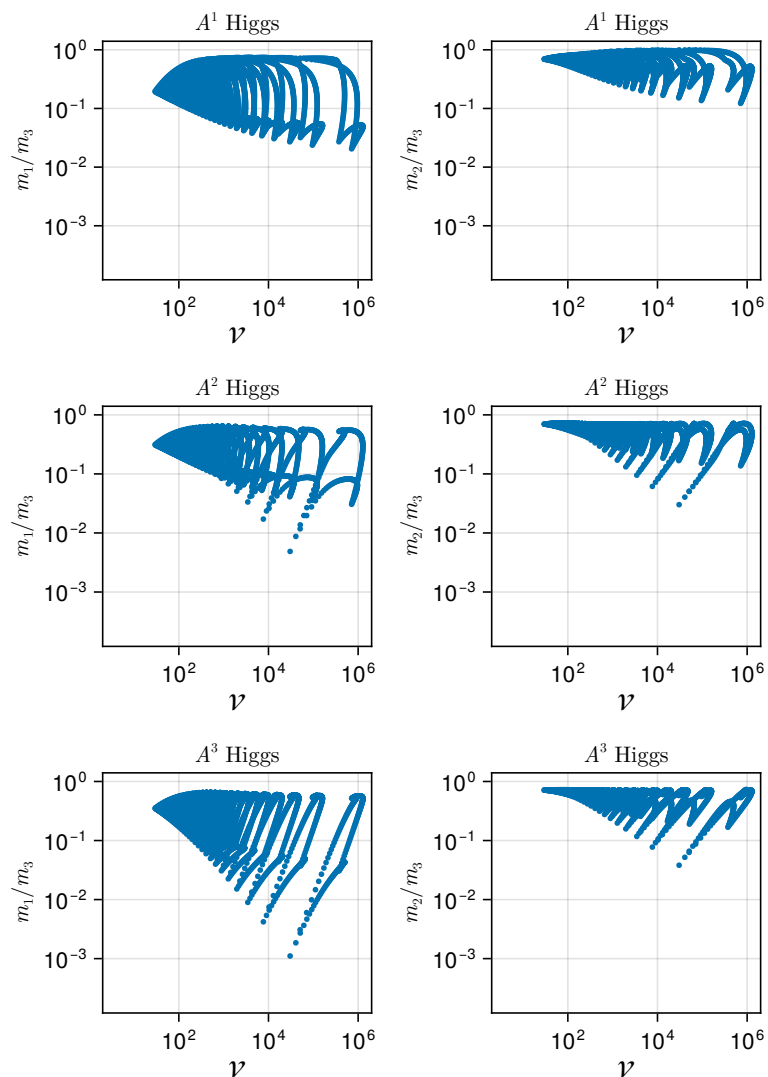


Figure 15: Mass ratios for CICY 7071 as a function of the minimum volume \mathcal{V} where all real parts of the moduli are greater than or equal to 1. The masses are ordered as $m_1 < m_2 < m_3$. The left (right) panel shows the scatter for m_1/m_3 (m_2/m_3).

- **Type 7 (CICY 7450)**

As an illustrative example of Type 7, we examine CICY 7450. The holomorphic Yukawa matrices are obtained from the intersection numbers as

$$\kappa_{ab1} = \begin{pmatrix} 0 & 0 & 0 \\ 0 & 0 & 4 \\ 0 & 4 & 8 \end{pmatrix}, \quad (\text{A.13})$$

when the Higgs field corresponds to A^1 ,

$$\kappa_{ab2} = \begin{pmatrix} 0 & 0 & 4 \\ 0 & 0 & 0 \\ 4 & 0 & 8 \end{pmatrix}, \quad (\text{A.14})$$

when the Higgs field corresponds to A^2 , and

$$\kappa_{ab3} = \begin{pmatrix} 0 & 4 & 8 \\ 4 & 0 & 8 \\ 8 & 8 & 8 \end{pmatrix}, \quad (\text{A.15})$$

when the Higgs field corresponds to A^3 .

Figure 16 shows the mass ratios m_1/m_3 and m_2/m_3 , which are obtained from eigenvalue ratios of $Y_{\hat{a}\hat{b}1}$, $Y_{\hat{a}\hat{b}2}$ and $Y_{\hat{a}\hat{b}3}$. The points correspond to discrete variations of the moduli ratio $T^1 : T^2 : T^3$, subject to the restriction $\text{Re} T^a \geq 1$. In this example, the (3×3) matrices $Y_{\hat{a}\hat{b}1}$ and $Y_{\hat{a}\hat{b}2}$ have rank 1. When the Higgs field corresponds to A^1 and A^2 , we have $m_1 = 0$ for any moduli values.

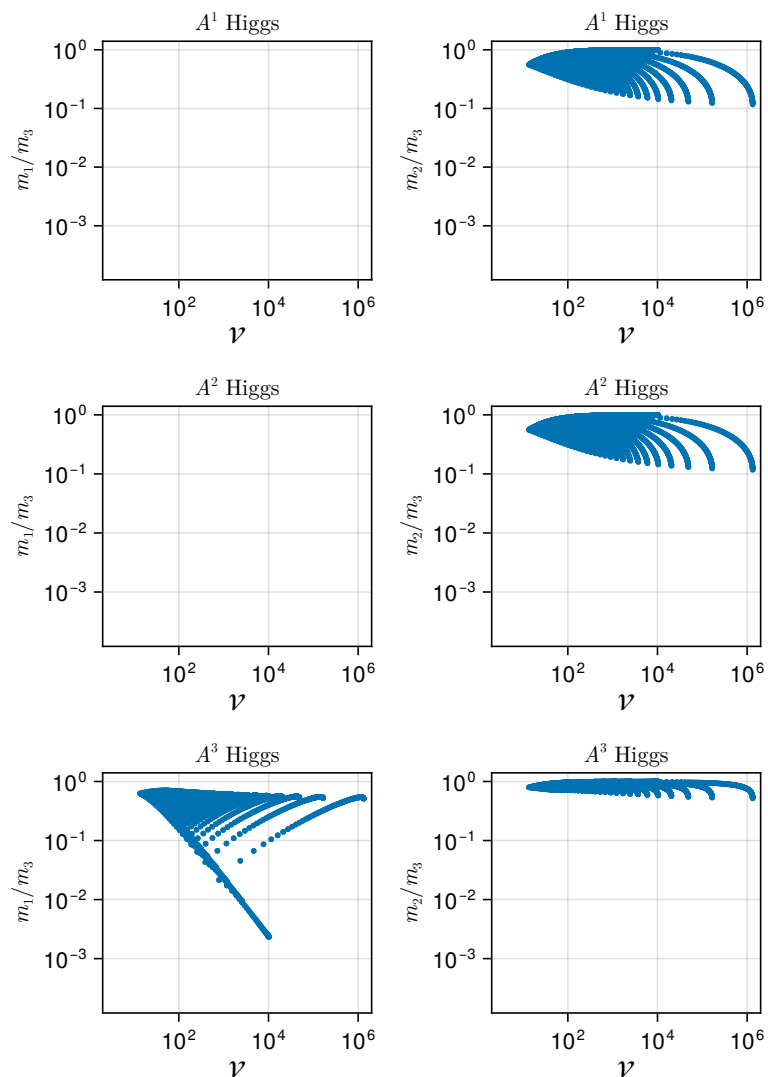


Figure 16: Mass ratios for CICY 7450 as a function of the minimum volume \mathcal{V} where all real parts of the moduli are greater than or equal to 1. The masses are ordered as $m_1 < m_2 < m_3$. The left (right) panel shows the scatter for m_1/m_3 (m_2/m_3).

- **Type 8 (CICY 7465)**

As an illustrative example of Type 8, we examine CICY 7465. The holomorphic Yukawa matrices are obtained from the intersection numbers as

$$\kappa_{ab1} = \begin{pmatrix} 0 & 0 & 0 \\ 0 & 0 & 4 \\ 0 & 4 & 8 \end{pmatrix}, \quad (\text{A.16})$$

when the Higgs field corresponds to A^1 ,

$$\kappa_{ab2} = \begin{pmatrix} 0 & 0 & 4 \\ 0 & 0 & 4 \\ 4 & 4 & 12 \end{pmatrix}, \quad (\text{A.17})$$

when the Higgs field corresponds to A^2 , and

$$\kappa_{ab3} = \begin{pmatrix} 0 & 4 & 8 \\ 4 & 4 & 12 \\ 8 & 12 & 8 \end{pmatrix}, \quad (\text{A.18})$$

when the Higgs field corresponds to A^3 .

Figure 17 shows the mass ratios m_1/m_3 and m_2/m_3 , which are obtained from eigenvalue ratios of $Y_{\hat{a}\hat{b}1}$, $Y_{\hat{a}\hat{b}2}$ and $Y_{\hat{a}\hat{b}3}$. The points correspond to discrete variations of the moduli ratio $T^1 : T^2 : T^3$, subject to the restriction $\text{Re} T^a \geq 1$. In this example, the (3×3) matrices $Y_{\hat{a}\hat{b}1}$ and $Y_{\hat{a}\hat{b}2}$ have rank 1. When the Higgs field corresponds to A^1 and A^2 , we have $m_1 = 0$ for any moduli values.

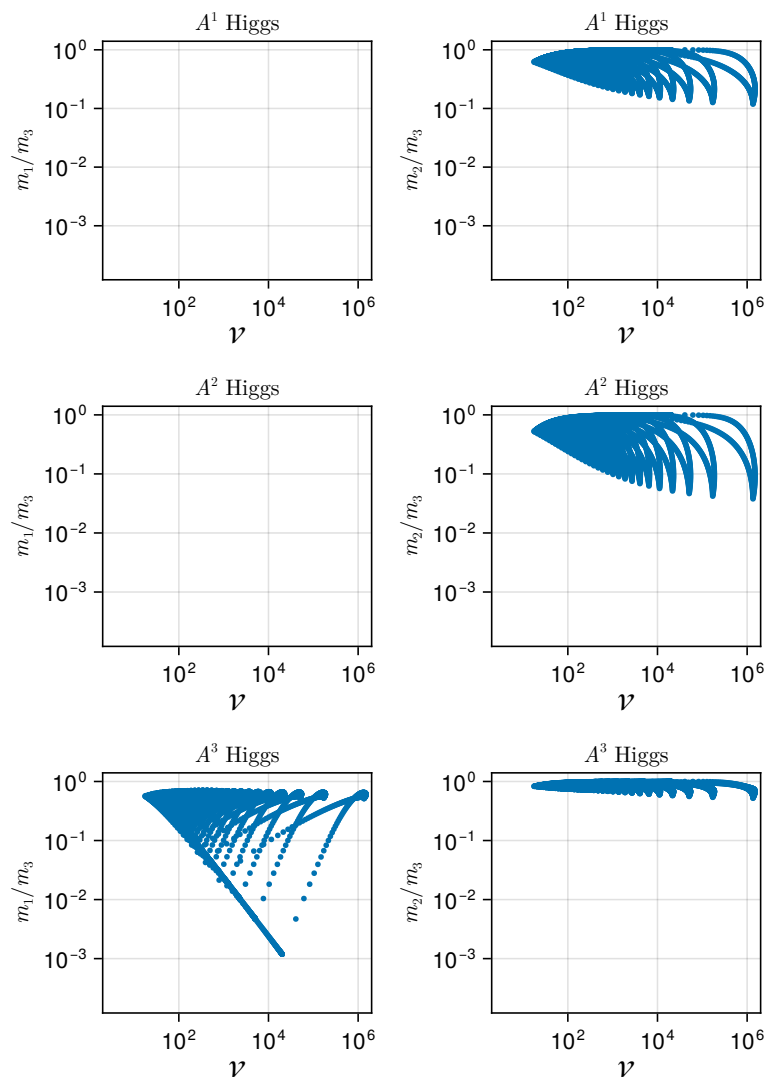


Figure 17: Mass ratios for CICY 7465 as a function of the minimum volume \mathcal{V} where all real parts of the moduli are greater than or equal to 1. The masses are ordered as $m_1 < m_2 < m_3$. The left (right) panel shows the scatter for m_1/m_3 (m_2/m_3).

- **Type 9 (CICY 7708)**

As an illustrative example of Type 9, we examine CICY 7708. The holomorphic Yukawa matrices are obtained from the intersection numbers as

$$\kappa_{ab1} = \begin{pmatrix} 0 & 0 & 0 \\ 0 & 2 & 5 \\ 0 & 5 & 2 \end{pmatrix}, \quad (\text{A.19})$$

when the Higgs field corresponds to A^1 ,

$$\kappa_{ab2} = \begin{pmatrix} 0 & 2 & 5 \\ 2 & 0 & 3 \\ 5 & 3 & 3 \end{pmatrix}, \quad (\text{A.20})$$

when the Higgs field corresponds to A^2 , and

$$\kappa_{ab3} = \begin{pmatrix} 0 & 5 & 2 \\ 5 & 3 & 3 \\ 2 & 3 & 0 \end{pmatrix}, \quad (\text{A.21})$$

when the Higgs field corresponds to A^3 .

Figure 18 shows the mass ratios m_1/m_3 and m_2/m_3 , which are obtained from eigenvalue ratios of $Y_{\hat{a}\hat{b}1}$, $Y_{\hat{a}\hat{b}2}$ and $Y_{\hat{a}\hat{b}3}$. The points correspond to discrete variations of the moduli ratio $T^1 : T^2 : T^3$, subject to the restriction $\text{Re } T^a \geq 1$. In this example, the (3×3) matrix $Y_{\hat{a}\hat{b}1}$ has rank 1. When the Higgs field corresponds to A^1 , we have $m_1 = 0$ for any moduli values.

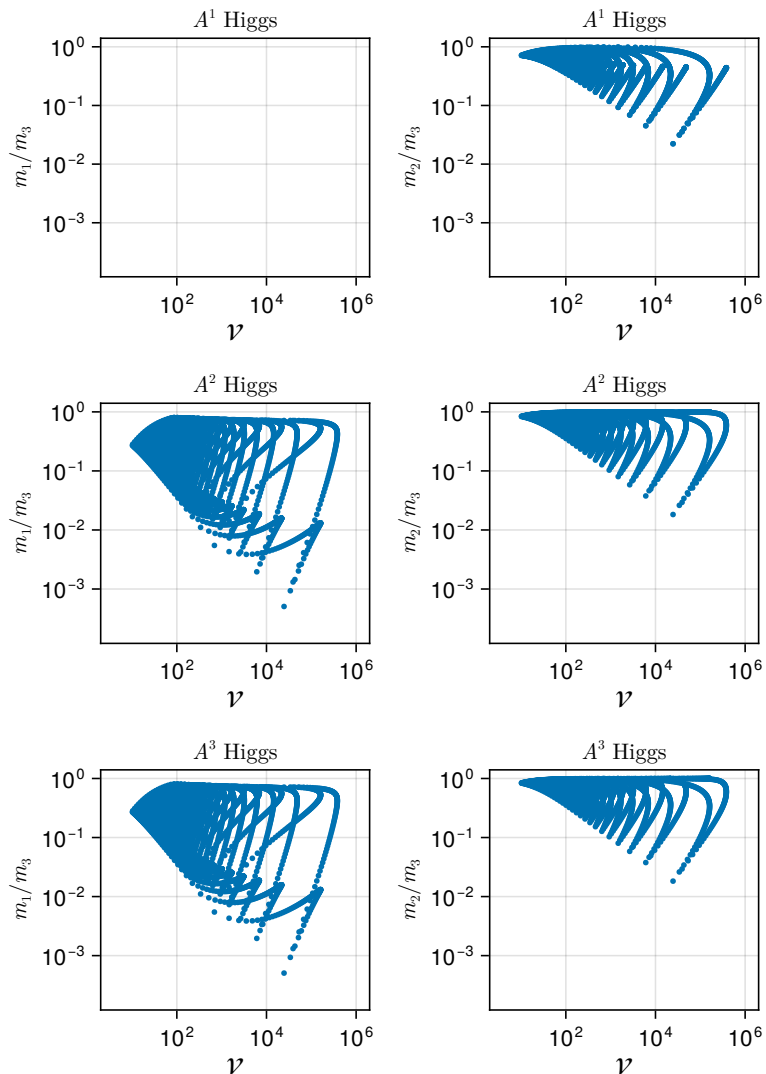


Figure 18: Mass ratios for CICY 7708 as a function of the minimum volume \mathcal{V} where all real parts of the moduli are greater than or equal to 1. The masses are ordered as $m_1 < m_2 < m_3$. The left (right) panel shows the scatter for m_1/m_3 (m_2/m_3).

• **Type 11 (CICY 7880)**

As an illustrative example of Type 11, we examine CICY 7880. The holomorphic Yukawa matrices are obtained from the intersection numbers as

$$\kappa_{ab1} = \begin{pmatrix} 0 & 0 & 0 \\ 0 & 0 & 3 \\ 0 & 3 & 2 \end{pmatrix}, \quad (\text{A.22})$$

when the Higgs field corresponds to A^1 ,

$$\kappa_{ab2} = \begin{pmatrix} 0 & 0 & 3 \\ 0 & 0 & 0 \\ 3 & 0 & 2 \end{pmatrix}, \quad (\text{A.23})$$

when the Higgs field corresponds to A^2 , and

$$\kappa_{ab3} = \begin{pmatrix} 0 & 3 & 2 \\ 3 & 0 & 2 \\ 2 & 2 & 0 \end{pmatrix}, \quad (\text{A.24})$$

when the Higgs field corresponds to A^3 .

Figure 19 shows the mass ratios m_1/m_3 and m_2/m_3 , which are obtained from eigenvalue ratios of $Y_{\hat{a}\hat{b}1}$, $Y_{\hat{a}\hat{b}2}$ and $Y_{\hat{a}\hat{b}3}$. The points correspond to discrete variations of the moduli ratio $T^1 : T^2 : T^3$, subject to the restriction $\text{Re} T^a \geq 1$. In this example, the (3×3) matrices $Y_{\hat{a}\hat{b}1}$ and $Y_{\hat{a}\hat{b}2}$ have rank 1. When the Higgs field corresponds to A^1 and A^2 , we have $m_1 = 0$ for any moduli values.

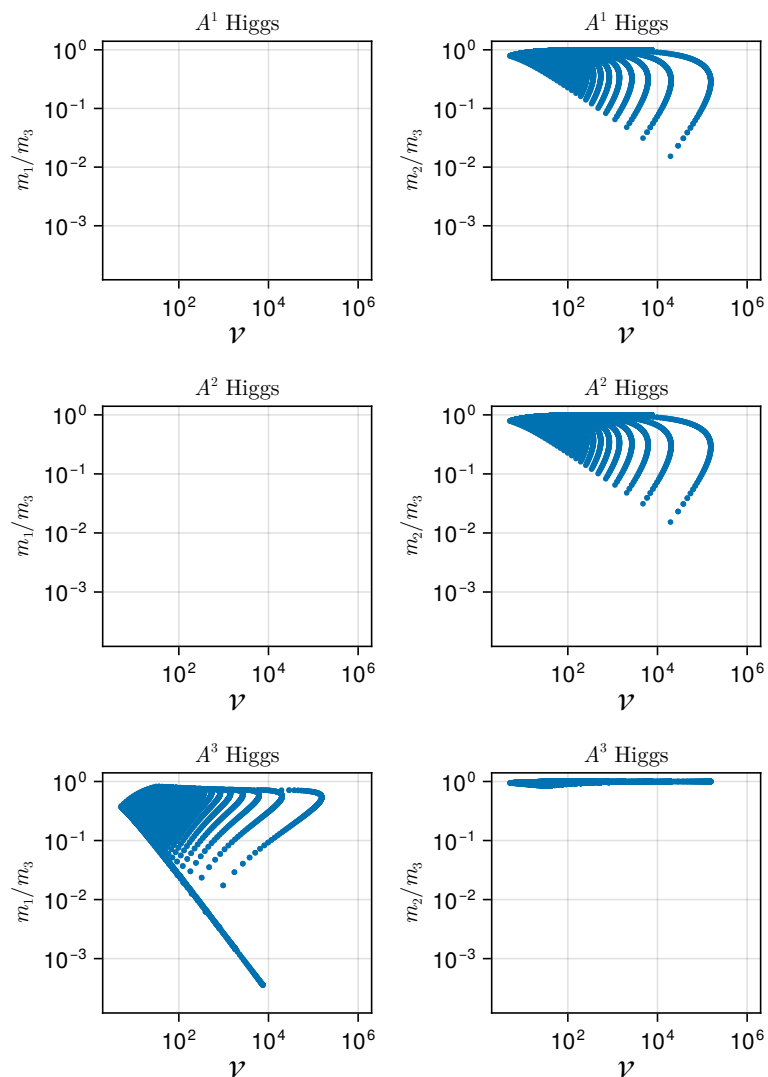


Figure 19: Mass ratios for CICY 7880 as a function of the minimum volume \mathcal{V} where all real parts of the moduli are greater than or equal to 1. The masses are ordered as $m_1 < m_2 < m_3$. The left (right) panel shows the scatter for m_1/m_3 (m_2/m_3).

References

- [1] R. Dijkgraaf, E.P. Verlinde and H.L. Verlinde, *C = 1 Conformal Field Theories on Riemann Surfaces*, *Commun. Math. Phys.* **115** (1988) 649.
- [2] T. Kobayashi, S. Raby and R.-J. Zhang, *Searching for realistic 4d string models with a Pati-Salam symmetry: Orbifold grand unified theories from heterotic string compactification on a Z(6) orbifold*, *Nucl. Phys. B* **704** (2005) 3 [[hep-ph/0409098](#)].
- [3] T. Kobayashi, H.P. Nilles, F. Ploger, S. Raby and M. Ratz, *Stringy origin of non-Abelian discrete flavor symmetries*, *Nucl. Phys. B* **768** (2007) 135 [[hep-ph/0611020](#)].

- [4] F. Beye, T. Kobayashi and S. Kuwakino, *Gauge Origin of Discrete Flavor Symmetries in Heterotic Orbifolds*, *Phys. Lett. B* **736** (2014) 433 [1406.4660].
- [5] H. Abe, K.-S. Choi, T. Kobayashi and H. Ohki, *Non-Abelian Discrete Flavor Symmetries from Magnetized/Intersecting Brane Models*, *Nucl. Phys. B* **820** (2009) 317 [0904.2631].
- [6] M. Berasaluce-Gonzalez, P.G. Camara, F. Marchesano, D. Regalado and A.M. Uranga, *Non-Abelian discrete gauge symmetries in 4d string models*, *JHEP* **09** (2012) 059 [1206.2383].
- [7] F. Marchesano, D. Regalado and L. Vazquez-Mercado, *Discrete flavor symmetries in D-brane models*, *JHEP* **09** (2013) 028 [1306.1284].
- [8] G. Altarelli and F. Feruglio, *Discrete Flavor Symmetries and Models of Neutrino Mixing*, *Rev. Mod. Phys.* **82** (2010) 2701 [1002.0211].
- [9] H. Ishimori, T. Kobayashi, H. Ohki, Y. Shimizu, H. Okada and M. Tanimoto, *Non-Abelian Discrete Symmetries in Particle Physics*, *Prog. Theor. Phys. Suppl.* **183** (2010) 1 [1003.3552].
- [10] T. Kobayashi, H. Ohki, H. Okada, Y. Shimizu and M. Tanimoto, *An Introduction to Non-Abelian Discrete Symmetries for Particle Physicists* (1, 2022), 10.1007/978-3-662-64679-3.
- [11] D. Hernandez and A.Y. Smirnov, *Lepton mixing and discrete symmetries*, *Phys. Rev. D* **86** (2012) 053014 [1204.0445].
- [12] S.F. King and C. Luhn, *Neutrino Mass and Mixing with Discrete Symmetry*, *Rept. Prog. Phys.* **76** (2013) 056201 [1301.1340].
- [13] S.F. King, A. Merle, S. Morisi, Y. Shimizu and M. Tanimoto, *Neutrino Mass and Mixing: from Theory to Experiment*, *New J. Phys.* **16** (2014) 045018 [1402.4271].
- [14] S.T. Petcov, *Discrete Flavour Symmetries, Neutrino Mixing and Leptonic CP Violation*, *Eur. Phys. J. C* **78** (2018) 709 [1711.10806].
- [15] J. Lauer, J. Mas and H.P. Nilles, *Duality and the Role of Nonperturbative Effects on the World Sheet*, *Phys. Lett. B* **226** (1989) 251.
- [16] J. Lauer, J. Mas and H.P. Nilles, *Twisted sector representations of discrete background symmetries for two-dimensional orbifolds*, *Nucl. Phys. B* **351** (1991) 353.
- [17] W. Lerche, D. Lust and N.P. Warner, *Duality Symmetries in $N = 2$ Landau-ginzburg Models*, *Phys. Lett. B* **231** (1989) 417.
- [18] S. Ferrara, D. Lust and S. Theisen, *Target Space Modular Invariance and Low-Energy Couplings in Orbifold Compactifications*, *Phys. Lett. B* **233** (1989) 147.
- [19] A. Baur, H.P. Nilles, A. Trautner and P.K.S. Vaudrevange, *Unification of Flavor, CP, and Modular Symmetries*, *Phys. Lett. B* **795** (2019) 7 [1901.03251].
- [20] H.P. Nilles, S. Ramos-Sánchez and P.K.S. Vaudrevange, *Eclectic Flavor Groups*, *JHEP* **02** (2020) 045 [2001.01736].
- [21] T. Kobayashi, S. Nagamoto, S. Takada, S. Tamba and T.H. Tatsuishi, *Modular symmetry and non-Abelian discrete flavor symmetries in string compactification*, *Phys. Rev. D* **97** (2018) 116002 [1804.06644].
- [22] T. Kobayashi and S. Tamba, *Modular forms of finite modular subgroups from magnetized D-brane models*, *Phys. Rev. D* **99** (2019) 046001 [1811.11384].

- [23] S. Kikuchi, T. Kobayashi and H. Uchida, *Modular flavor symmetries of three-generation modes on magnetized toroidal orbifolds*, *Phys. Rev. D* **104** (2021) 065008 [2101.00826].
- [24] H. Ohki, S. Uemura and R. Watanabe, *Modular flavor symmetry on a magnetized torus*, *Phys. Rev. D* **102** (2020) 085008 [2003.04174].
- [25] S. Kikuchi, T. Kobayashi, S. Takada, T.H. Tatsuishi and H. Uchida, *Revisiting modular symmetry in magnetized torus and orbifold compactifications*, *Phys. Rev. D* **102** (2020) 105010 [2005.12642].
- [26] S. Kikuchi, T. Kobayashi, H. Otsuka, S. Takada and H. Uchida, *Modular symmetry by orbifolding magnetized $T^2 \times T^2$: realization of double cover of Γ_N* , *JHEP* **11** (2020) 101 [2007.06188].
- [27] Y. Almumin, M.-C. Chen, V. Knapp-Pérez, S. Ramos-Sánchez, M. Ratz and S. Shukla, *Metaplectic Flavor Symmetries from Magnetized Tori*, *JHEP* **05** (2021) 078 [2102.11286].
- [28] K. Ishiguro, T. Kai, H. Okada and H. Otsuka, *Flavor, CP and metaplectic modular symmetries in Type IIB chiral flux vacua*, *JHEP* **12** (2023) 136 [2305.19155].
- [29] S. Kikuchi, T. Kobayashi, K. Nasu, S. Takada and H. Uchida, *Modular symmetry in magnetized T^{2g} torus and orbifold models*, 2309.16447.
- [30] T. Kobayashi and S. Nagamoto, *Zero-modes on orbifolds : magnetized orbifold models by modular transformation*, *Phys. Rev. D* **96** (2017) 096011 [1709.09784].
- [31] A. Strominger, *SPECIAL GEOMETRY*, *Commun. Math. Phys.* **133** (1990) 163.
- [32] P. Candelas and X. de la Ossa, *Moduli Space of Calabi-Yau Manifolds*, *Nucl. Phys. B* **355** (1991) 455.
- [33] K. Ishiguro, T. Kobayashi and H. Otsuka, *Spontaneous CP violation and symplectic modular symmetry in Calabi-Yau compactifications*, *Nucl. Phys. B* **973** (2021) 115598 [2010.10782].
- [34] K. Ishiguro, T. Kobayashi and H. Otsuka, *Symplectic modular symmetry in heterotic string vacua: flavor, CP, and R-symmetries*, *JHEP* **01** (2022) 020 [2107.00487].
- [35] F. Feruglio, *Are neutrino masses modular forms?*, in *From My Vast Repertoire ...: Guido Altarelli's Legacy*, A. Levy, S. Forte and G. Ridolfi, eds., pp. 227–266 (2019), DOI [1706.08749].
- [36] T. Kobayashi, K. Tanaka and T.H. Tatsuishi, *Neutrino mixing from finite modular groups*, *Phys. Rev. D* **98** (2018) 016004 [1803.10391].
- [37] J.T. Penedo and S.T. Petcov, *Lepton Masses and Mixing from Modular S_4 Symmetry*, *Nucl. Phys. B* **939** (2019) 292 [1806.11040].
- [38] P.P. Novichkov, J.T. Penedo, S.T. Petcov and A.V. Titov, *Modular A_5 symmetry for flavour model building*, *JHEP* **04** (2019) 174 [1812.02158].
- [39] T. Kobayashi, N. Omoto, Y. Shimizu, K. Takagi, M. Tanimoto and T.H. Tatsuishi, *Modular A_4 invariance and neutrino mixing*, *JHEP* **11** (2018) 196 [1808.03012].
- [40] T. Kobayashi and M. Tanimoto, *Modular flavor symmetric models*, *Int. J. Mod. Phys. A* **39** (2024) 2441012 [2307.03384].
- [41] G.-J. Ding and S.F. King, *Neutrino mass and mixing with modular symmetry*, *Rept. Prog. Phys.* **87** (2024) 084201 [2311.09282].

- [42] A. Font, L.E. Ibanez, H.P. Nilles and F. Quevedo, *On the Concept of Naturalness in String Theories*, *Phys. Lett. B* **213** (1988) 274.
- [43] M. Cvetič, *Suppression of Nonrenormalizable Terms in the Effective Superpotential for (Blowup) Orbifold Compactification*, *Phys. Rev. Lett.* **59** (1987) 1795.
- [44] T. Kobayashi, S.L. Parameswaran, S. Ramos-Sanchez and I. Zavala, *Revisiting Coupling Selection Rules in Heterotic Orbifold Models*, *JHEP* **05** (2012) 008 [1107.2137].
- [45] L.J. Dixon, J.A. Harvey, C. Vafa and E. Witten, *Strings on Orbifolds. 2.*, *Nucl. Phys. B* **274** (1986) 285.
- [46] S. Hamidi and C. Vafa, *Interactions on Orbifolds*, *Nucl. Phys. B* **279** (1987) 465.
- [47] L.J. Dixon, D. Friedan, E.J. Martinec and S.H. Shenker, *The Conformal Field Theory of Orbifolds*, *Nucl. Phys. B* **282** (1987) 13.
- [48] T. Kobayashi and N. Ohtsubo, *Yukawa Coupling Condition of $Z(N)$ Orbifold Models*, *Phys. Lett. B* **245** (1990) 441.
- [49] T. Kobayashi and N. Ohtsubo, *Geometrical aspects of $Z(N)$ orbifold phenomenology*, *Int. J. Mod. Phys. A* **9** (1994) 87.
- [50] T. Kobayashi, *Selection rules for nonrenormalizable couplings in superstring theories*, *Phys. Lett. B* **354** (1995) 264 [hep-ph/9504371].
- [51] J.J. Heckman, J. McNamara, M. Montero, A. Sharon, C. Vafa and I. Valenzuela, *On the Fate of Stringy Non-Invertible Symmetries*, 2402.00118.
- [52] J. Kaidi, Y. Tachikawa and H.Y. Zhang, *On a class of selection rules without group actions in field theory and string theory*, *SciPost Phys.* **17** (2024) 169 [2402.00105].
- [53] T. Kobayashi, R. Nishida and H. Otsuka, *Non-Invertible Selection Rules on Heterotic Non-Abelian Orbifolds*, 2509.10019.
- [54] T. Kobayashi and H. Otsuka, *Non-invertible flavor symmetries in magnetized extra dimensions*, *JHEP* **11** (2024) 120 [2408.13984].
- [55] S. Funakoshi, T. Kobayashi and H. Otsuka, *Quantum aspects of non-invertible flavor symmetries in intersecting/magnetized D-brane models*, *JHEP* **04** (2025) 183 [2412.12524].
- [56] T. Kobayashi, H. Otsuka and M. Tanimoto, *Yukawa textures from non-invertible symmetries*, *JHEP* **12** (2024) 117 [2409.05270].
- [57] T. Kobayashi, Y. Nishioka, H. Otsuka and M. Tanimoto, *More about quark Yukawa textures from selection rules without group actions*, *JHEP* **05** (2025) 177 [2503.09966].
- [58] T. Kobayashi, H. Otsuka, M. Tanimoto and H. Uchida, *Lepton mass textures from non-invertible multiplication rules*, *JHEP* **08** (2025) 189 [2505.07262].
- [59] Z. Jiang, B.-Y. Qu and G.-J. Ding, *Texture-zeros in minimal seesaw from noninvertible symmetry fusion rules*, *Phys. Rev. D* **112** (2025) 115029 [2510.07236].
- [60] Q. Liang and T.T. Yanagida, *Non-invertible symmetry as an axion-less solution to the strong CP problem*, *Phys. Lett. B* **868** (2025) 139706 [2505.05142].
- [61] T. Kobayashi, H. Otsuka and T.T. Yanagida, *Non-invertible Symmetry as a Solution to the Strong CP Problem in a GUT-inspired Standard Model*, 2508.12287.

- [62] T. Kobayashi, H. Otsuka, M. Tanimoto and T.T. Yanagida, *GUT-motivated non-invertible symmetry as a solution to the strong CP problem and the neutrino CP-violating phase*, 2510.01680.
- [63] T. Kobayashi, H. Okada and H. Otsuka, *Radiative neutrino mass models from non-invertible selection rules*, *JHEP* **12** (2025) 111 [2505.14878].
- [64] T. Nomura and H. Okada, *Radiative lepton seesaw model in a non-invertible fusion rule and gauged $B - L$ symmetry*, 2506.16706.
- [65] J. Chen, C.-Q. Geng, H. Okada and J.-J. Wu, *A radiative lepton model in a non-invertible fusion rule*, 2507.11951.
- [66] H. Okada and Y. Shigekami, *Three-loop induced neutrino mass model in a non-invertible symmetry*, 2507.16198.
- [67] Y. Nakai, H. Otsuka, Y. Shigekami and Z. Zhang, *The Minimal Supersymmetric Standard Model with Non-Invertible Selection Rules*, 2512.21509.
- [68] M. Suzuki and L.-X. Xu, *Phenomenological implications of a class of non-invertible selection rules*, 2503.19964.
- [69] T. Kobayashi, H. Mita, H. Otsuka and R. Sakuma, *Matter symmetries in supersymmetric standard models from non-invertible selection rules*, 2506.10241.
- [70] P. Candelas, G.T. Horowitz, A. Strominger and E. Witten, *Vacuum configurations for superstrings*, *Nucl. Phys. B* **258** (1985) 46.
- [71] A. Constantin, C.S. Fraser-Taliente, T.R. Harvey, A. Lukas and B. Ovrut, *Computation of quark masses from string theory*, *Nucl. Phys. B* **1010** (2025) 116778 [2402.01615].
- [72] A. Constantin, L.T.Y. Leung, A. Lukas and L.A. Nutricati, *Reproducing Standard Model fermion masses and mixing in string theory: A heterotic line bundle study*, *Phys. Rev. D* **113** (2026) 046005 [2507.03076].
- [73] C.D. Froggatt and H.B. Nielsen, *Hierarchy of Quark Masses, Cabibbo Angles and CP Violation*, *Nucl. Phys. B* **147** (1979) 277.
- [74] J. Dong, T. Kobayashi, R. Nishida, S. Nishimura and H. Otsuka, *Coupling selection rules in heterotic Calabi-Yau compactifications*, *JHEP* **09** (2025) 012 [2504.09773].
- [75] L.J. Dixon, V. Kaplunovsky and J. Louis, *On Effective Field Theories Describing $(2,2)$ Vacua of the Heterotic String*, *Nucl. Phys. B* **329** (1990) 27.
- [76] A. Strominger and E. Witten, *New Manifolds for Superstring Compactification*, *Commun. Math. Phys.* **101** (1985) 341.
- [77] P. Candelas, *Yukawa Couplings Between $(2,1)$ Forms*, *Nucl. Phys. B* **298** (1988) 458.
- [78] P. Candelas, A.M. Dale, C.A. Lutken and R. Schimmrigk, *Complete Intersection Calabi-Yau Manifolds*, *Nucl. Phys. B* **298** (1988) 493.
- [79] P. Candelas, C.A. Lutken and R. Schimmrigk, *COMPLETE INTERSECTION CALABI-YAU MANIFOLDS. 2. THREE GENERATION MANIFOLDS*, *Nucl. Phys. B* **306** (1988) 113.
- [80] P.S. Green, T. Hubsch and C.A. Lutken, *All Hodge Numbers of All Complete Intersection Calabi-Yau Manifolds*, *Class. Quant. Grav.* **6** (1989) 105.

- [81] A.-m. He and P. Candelas, *On the Number of Complete Intersection Calabi-Yau Manifolds*, *Commun. Math. Phys.* **135** (1990) 193.
- [82] M. Gagnon and Q. Ho-Kim, *An Exhaustive list of complete intersection Calabi-Yau manifolds*, *Mod. Phys. Lett. A* **9** (1994) 2235.
- [83] L.B. Anderson, Y.-H. He and A. Lukas, *Monad Bundles in Heterotic String Compactifications*, *JHEP* **07** (2008) 104 [0805.2875].
- [84] <https://www.thphys.physics.ox.ac.uk/projects/CalabiYau/cicylist/cicylist.txt>.
- [85] S. Weinberg, *The Problem of Mass*, *Trans. New York Acad. Sci.* **38** (1977) 185.
- [86] K. Ishiguro, T. Kobayashi and H. Otsuka, *Hierarchical structure of physical Yukawa couplings from matter field Kähler metric*, *JHEP* **07** (2021) 064 [2103.10240].
- [87] S. Antusch, K. Hinze and S. Saad, *Updated Running Quark and Lepton Parameters at Various Scales*, 2510.01312.
- [88] R. Barbieri, G. Isidori, J. Jones-Perez, P. Lodone and D.M. Straub, *$U(2)$ and Minimal Flavour Violation in Supersymmetry*, *Eur. Phys. J. C* **71** (2011) 1725 [1105.2296].
- [89] G. Blankenburg, G. Isidori and J. Jones-Perez, *Neutrino Masses and LFV from Minimal Breaking of $U(3)^5$ and $U(2)^5$ flavor Symmetries*, *Eur. Phys. J. C* **72** (2012) 2126 [1204.0688].
- [90] R. Barbieri, D. Buttazzo, F. Sala and D.M. Straub, *Flavour physics from an approximate $U(2)^3$ symmetry*, *JHEP* **07** (2012) 181 [1203.4218].
- [91] J. Fuentes-Martín, G. Isidori, J. Pagès and K. Yamamoto, *With or without $U(2)$? Probing non-standard flavor and helicity structures in semileptonic B decays*, *Phys. Lett. B* **800** (2020) 135080 [1909.02519].
- [92] M. Bershadsky, S. Cecotti, H. Ooguri and C. Vafa, *Kodaira-Spencer theory of gravity and exact results for quantum string amplitudes*, *Commun. Math. Phys.* **165** (1994) 311 [hep-th/9309140].
- [93] T. Kobayashi and H. Otsuka, *On stringy origin of minimal flavor violation*, *Eur. Phys. J. C* **82** (2022) 25 [2108.02700].
- [94] T. Kobayashi, H. Otsuka, M. Tanimoto and K. Yamamoto, *Modular symmetry in the SMEFT*, *Phys. Rev. D* **105** (2022) 055022 [2112.00493].
- [95] T. Kobayashi, H. Otsuka, M. Tanimoto and K. Yamamoto, *Lepton flavor violation, lepton $(g - 2)_{\mu,e}$ and electron EDM in the modular symmetry*, *JHEP* **08** (2022) 013 [2204.12325].
- [96] L.-J. Kang, H. Sun and J.-H. Yu, *Complete Operator Basis for the modular invariant SMEFT*, 2601.23060.
- [97] K. Hoshiya, S. Kikuchi, T. Kobayashi and H. Uchida, *Quark and lepton flavor structure in magnetized orbifold models at residual modular symmetric points*, *Phys. Rev. D* **106** (2022) 115003 [2209.07249].
- [98] L. Kofman, A.D. Linde, X. Liu, A. Maloney, L. McAllister and E. Silverstein, *Beauty is attractive: Moduli trapping at enhanced symmetry points*, *JHEP* **05** (2004) 030 [hep-th/0403001].
- [99] S. Kikuchi, T. Kobayashi, K. Nasu and Y. Yamada, *Moduli trapping mechanism in modular flavor symmetric models*, *JHEP* **08** (2023) 081 [2307.13230].